



Selection of Sensitive Post-Stack and Pre-Stack Seismic Inversion Attributes for Improved Characterization of Thin Gas-Bearing Sands

UROOJ SHAKIR,^{1,2} AAMIR ALI,¹  MUYASSAR HUSSAIN,¹ TAHIR AZEEM,¹ and LAMUAIL BASHIR³

Abstract—The mapping and characterization of thin gas sand layers have always been a challenge through conventional seismic interpretation procedures. Seismic inversion techniques have been effectively applied to evaluate the hydrocarbon reservoirs with high heterogeneity and deep burial depth with thicknesses below seismic resolution. In this study, thin gas sand layers of the Lower Ranikot Formation of the Mehar gas field in the Kirthar Fold Belt, Pakistan, have been characterized via the application of sensitive post-stack model-based seismic inversion (PMBSI) and pre-stack simultaneous seismic inversion (PSSI). These sands are producing in the nearby fields; however, their potential is still untapped in the study area, which needs to be explored for further development. In order to evaluate the gas potential, petrophysical analysis demarcated three gas-bearing zones within the targeted reservoir. The spatial extent of these identified sand packages has been evaluated in detail by the application of the above selected seismic inversion techniques. The results of PMBSI depicted low impedance values within the sand layers of the Lower Ranikot Formation, but PSSI efficaciously separated the thin gas-bearing and non-bearing sand intervals. Furthermore, the impedance-derived porosities predicted via probabilistic neural network (PNN) show excellent agreement with the computed porosities from interpreted well logs and at producing blind wells. The techniques adopted to delineate and map the potential thin gas sands of the Mehar gas field may be very fruitful and adequate for basins with similar geological settings.

Keywords: Petrophysics, model-based seismic inversion, simultaneous seismic inversion, probabilistic neural network, V_p/V_s ratio.

1. Introduction

Improved reservoir characterization provides the foundation to determine the real economic potential

of any exploration field. A detailed analysis of the static and dynamic behavior of hydrocarbon reservoirs with the integration of multiple data sets is essential for field development and to reduce uncertainty in defining new drilling locations (Torres-Verdín et al., 2004; Karbalaali et al., 2013; Ali et al., 2018). Seismic sections are layer interface impedance outputs with band-limited traces, missing low-frequency information (Yilmaz, 2001; Torres-Verdín et al., 2004; Prskalo, 2007; Karbalaali et al., 2013), so it is difficult to construct an accurate subsurface model based on a single data set (Karim et al., 2016; Nawaz, 2013). The accuracy can be improved by integrating different data sets, including well and seismic data (Robinson and Silvia, 1978; Hampson et al., 2005; Swisi, 2009). In this regard, seismic inversion bridges the gap between these two data sets and has become a standard component for improved reservoir characterization (Azeem et al., 2018; Sams & Saussus, 2013; Sams et al., 2011).

Nowadays, several inversion techniques are applied, and the selection of each depends on the available data set and existing problem (Azeem et al., 2017; Clochard et al., 2009; Nawaz, 2013; Russell, 1999). Post-stack inversion provides acoustic impedance, assuming zero offset reflectivity, while pre-stack involves the angle gathers. In post-stack, the complete seismic volume is resolved into one attribute, p -impedance (Z_p) (Eidsvik et al., 2004; Sams & Saussus, 2007), while pre-stack provides a variety of attributes such as Z_p , s -impedance (Z_s), and density (ρ) (Pendrel et al., 2017). When the estimation of multiple reservoir parameters based on a single attribute (Z_p) does not provide satisfactory output (Coléou et al., 2005; Kalkomey, 1997; Ødegaard & Avseth, 2004), then a technique considering the

¹ Department of Earth Sciences, Quaid-i-Azam University, Islamabad 45320, Pakistan. E-mail: aamirali.geo@gmail.com; aakgeo82@qau.edu.pk

² Department of Earth and Environmental Sciences, Bahria University, Islamabad, Pakistan.

³ CGG Services SAS, Abu Dhabi, UAE.

offset-preserved angular amplitude of seismic data is utilized to accurately separate the litho-fluid content in the complex scenarios (Oliver, 2008). However, it requires global wavelets and background models (Barone & Sen, 2015). The ultimate task of the seismic inversion technique is to determine the reservoir properties of interest over the whole seismic volume through statistical or empirical relationships developed between elastic and petrophysical properties (Doyen et al., 1989; Hampson et al., 2005).

The Kirthar Fold Belt (KFB) is recognized as a major catchment basin due to its versatile structural style and hydrocarbon accumulation. Because of its complex tectonic history and variable geology, several clastic reservoirs have been explored here. Among them is the Ranikot Formation of the Paleocene age, which many companies have tapped as a hydrocarbon potential reservoir. However, the lower part of the Ranikot Formation contains thin beds of sand facies which needs to be explored as a prospect. This study mainly focuses on the implications of inverted results to investigate and locate the most reliable hydrocarbon-bearing strata and new fairways of those thin sand beds. Conventional analysis using basic techniques has been carried out by many researchers to evaluate the reservoir potential of the abovementioned formation (Hinsch et al., 2018; Zafar et al., 2018), but advanced selective inversion algorithms have not been performed yet in detail to delineate the thin sand beds of Lower Ranikot. In this paper, the authors have successfully resolved this issue by using advanced and sensitive seismic inversion algorithms.

2. Geological Settings

Geologically, the study area (Mehtar Block) is part of the KFB. The KFB is a 150–200 km-wide, northeast-trending, east-verging deformation zone bounded by the Sulaiman Fold-and-Thrust Belt in the north, Chaman Fault in the west, Kirthar Foredeep in the east, and Indus Delta in the south (Fig. 1). The Kirthar Foredeep is considered a significant kitchen for oil and gas generation in the KFB (Szeliga et al., 2009) and is divided into eastern, central, and western parts (Ahmad et al., 2012; Besse & Courtillot, 1988;

Patriat & Achache, 1984; Searle et al., 1997). The Kirthar Foredeep hosts several fields, including Bhit, Badhra, Zamzama, Rehmat, Gambat, Miano, Mehtar, and Mazarani, producing from Cretaceous/Tertiary reservoirs (Ahmad et al., 2004; Arshad et al., 2013; Mahmud & Aziz, 2002). However, the Late Cretaceous Pab Sandstone and Early Paleocene Lower Ranikot Formation are the primary target reservoirs in the southern KFB and adjacent foredeep areas (Fitzsimmons et al., 2005). The uplifting of the emergent Indian continent in the Early Cretaceous age triggered the deposition of sediments in the passive margin settings. As a result of the uplift, thick deposition of Sembar and Lower Goru formations took place along the passive margin, acting as a primary source for the above lying sand reservoirs (Ahmad et al., 2004; Bender & Raza, 1995; Richard et al., 2001). The sands of the Lower Ranikot Formation were also deposited in these environments (Arshad et al., 2013), which is the main target reservoir in the area under study.

Significant variations in lithology of the Lower Ranikot Formation represents mixed carbonate-siliciclastic litho-facies, which can be divided into three units: the lower division is carbonate-dominant towards the north and siliciclastic towards the south, the middle division is dominated by offshore muds and shale, and the upper-division contains sand units coarsening upward towards the north–northeast and are offshore mud dominated towards the south–southwest (Fig. 2; Ahmad & Ahmad, 2005; Hinsch et al., 2018; Zafar et al., 2018).

3. Data Set and Methodology

The data set used in this study includes three wells (Mehtar-01, 02, and 03), 3D post- and pre-stack seismic data, along with root mean square (RMS) stacking velocities. Post-stack seismic data was processed following the complete processing steps starting from geometry assignment, static correction, deconvolution (to enhance temporal resolution and multiple removals), normal moveout (NMO) correction (to remove the offset effects) until migration. First, post-stack and later pre-stack time migration was performed to resolve the complex geometries,

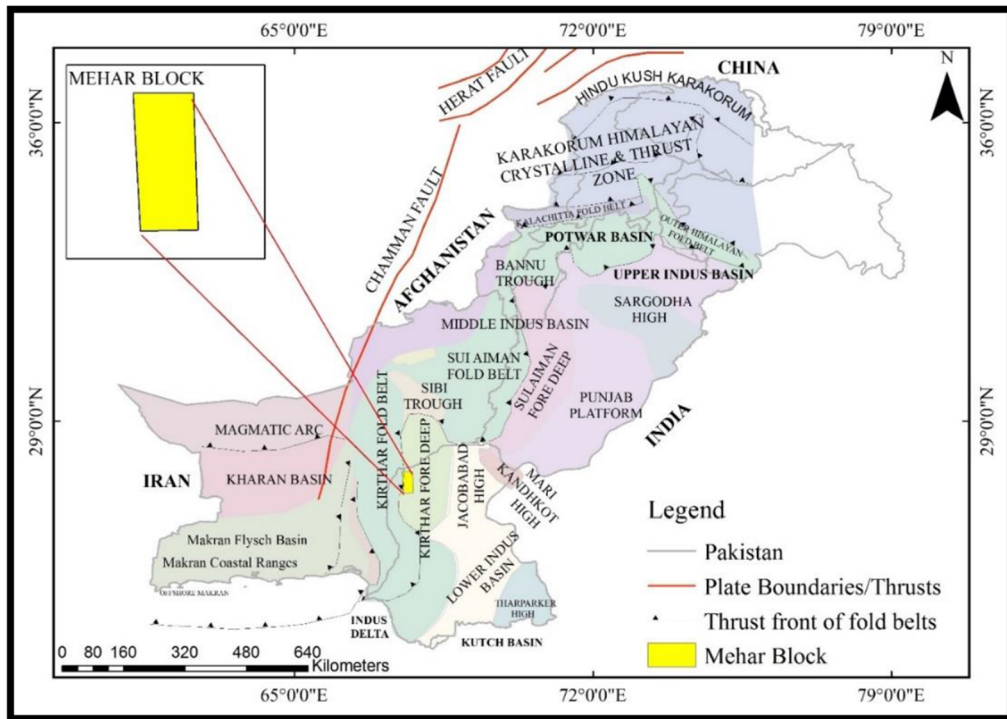









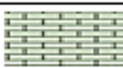


Figure 1

Tectonic map of Pakistan with marked thrust boundaries and fold belts. The rectangle highlighted in yellow represents the Mehar block boundary

and finally, the data were converted to the final stack. The pre-stack seismic data was divided into three offset stacks (near, mid and far) and later converted to an angle stack (near, mid, far) by using RMS velocities. The details of processing parameters are tabulated in Table 1. The extent of the 3D seismic cube along with the well locations is shown in Fig. 3. Well data include complete log suites of gamma-ray (GR), caliper (CALI), spontaneous potential (SP), sonic logs (DT4P, DT4S), neutron porosity (NPHI), resistivity (LLS, MSFL and LLD), and density (RHOB). The Sofiya-01, 02 and Mehar-05 wells producing from the same reservoir are used as blind wells to validate the final outputs. All three wells penetrate the primary target, i.e., Lower Ranikot, while Mehar-02 and 03 also reach the secondary reservoir, i.e., Pab Sandstone.

This present study was performed in three phases. In the first phase, seismic interpretation was performed to delineate the subsurface target horizons and structural geometries. The horizons were

identified after establishing a time-to-depth relationship with the help of well log data. Potential gas-bearing sand intervals were identified after performing petrophysical analysis based on well log data. The interpreted seismic horizons and elastic logs (sonic and density) are necessary inputs to perform any type of seismic inversion process. Figure 4 shows the workflow adopted to perform two types of seismic inversions. Zero offset final stacked seismic was utilized in post-stack inversion, while near, mid, and far angle stacks were used as an input parameter in pre-stack seismic inversion. Initial steps of wavelet extraction, well to seismic tie and low-frequency model are identical in both post- and pre-stack seismic inversions. First, a statistical wavelet was extracted from seismic data, and seismic-to-well tie was carried out. Later, to optimize the correlation to the maximum confidence level, a well-based wavelet was utilized. A low-frequency acoustic-impedance model (initial model) was generated and added via

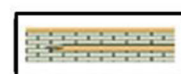
Age	Form	Member	source	Depth	Lithology		Hydrocarbon occurrences	
					West	East		
PLIOCENE	Upper	Swalik Group	SWALIK					
								
OLIGOCENE		NARI						MARI QADIRPUR SUI, KANDHKOT QADIRPUR, SUI KADHKOT, SURI SUI, UCH KANDHKOT QADIRPUR, KANORA KHAIRPUR, SURI LOTI, BADAR MAZARANI
EOCENE	Middle Upper	Kirthar	ORAZINDA		1000			
			PIPKOH					
			SIRKI					
			HABIB RAHI					
	Lower	Leki	GHAZU SHALE					
			SUI UPPER					
			SUI SHALE					
		SUI MAIN						
PALAEOCENE	Rerikot	DUNGHAN						
		UPPER RANIKOT						
		LOWER RANIKOT						
CRETACEOUS	Upper	Pab	PAB		2000			
		Mughal kot	Mughal Kot					
	Middle	Parh	PARH					
	Lower	GORU	UPPER GURU		3000			
			LOWER	GS30				
			GS20					
		GS10						
	Sembar	SEMBAR						
	JURASSIC	MIDDLE	CHILTAN			CHILTAN		4000



Sandstone, Shale and Conglomerate



Shale and Sandstone



Limestone and Shale



Limestone



Shale with Interbedded Sandstone



Shale and Marl

◀Figure 2

Generalized stratigraphical column of the Central Indus Basin with different hydrocarbon fields in the last column (Khan et al., 2017). The legend represents different lithologies present in this basin

interpreted seismic input to compensate for missing low frequencies.

In the second phase, model-based post-stack seismic inversion (PMBSI) was performed because of its reliable algorithm that deciphers the geological boundaries and structural trends with limited seismic data quality and fewer wells. Each well was correlated with seismic data, and inversion analysis was performed to reduce the error up to the optimum level and to determine the inversion parameters. Finally, PMBSI is applied over the whole seismic volume to give an inverted Z_p attribute (Fig. 4a).

Z_p depicted low impedances at the reservoir level, potential gas-bearing thin sand layers still were not resolved. In the third phase, to delineate thin sand packages with fluid presence (sweet spots), pre-stack simultaneous seismic inversion (PSSI) was performed. The available three individual offset stacks were converted into angle stacks (near, mid, far) by using suitable velocities to generate super-gather

seismic data used as an input in PSSI. The statistical wavelet was extracted from the super-gather initially. Then after establishing the initial well tie, a well-based wavelet was utilized to optimize the well-to-seismic tie as performed earlier for PMBSI. Afterwards, cross-plot analysis was carried out in which different elastic and petrophysical properties were utilized to analyze the petro-elastic response against the fluid presence. Based on the sensitivity of the elastic attributes, PSSI was chosen for detailed analysis. Again, inversion analysis was run iteratively, and parameters to perform the inversion were optimized. Finally, inversion was performed over the entire seismic volume with outputs in the form of inverted Z_p , Z_s and V_p/V_s ratio (Fig. 4b).

In the last step, impedances were converted in porosity cubes via a non-linear probabilistic neural network (PNN) approach. The porosity was derived from the empirical relationship between the actual and predicted porosities at well locations and extrapolated over the entire seismic volume. In this technique, petrophysical properties estimated from all the wells were trained by taking post-stack seismic attributes as internal attributes and inverted elastic properties as external attributes.

Table 1

Details of seismic processing parameters applied on Mehar gas field data

<i>Mehar 3D seismic processing parameters</i>	
Common mid-point interval: 30 m	Final datum: 0 m
Processing sample interval: 2 ms	Replacement velocity: 1800 m/s
Start time: 0 ms	
Trace length: 5000 ms	
<i>Processing sequence</i>	
1-Reformat	14-2nd pass velocity analysis (every 600 m)/residual statics
2-Geometry application	15-3rd pass velocity analysis (every 600 m)/residual statics
3-Grid define	16-Pre-stack 4D random noise attenuation
4-Bad trace editing	17-4th pass velocity analysis (every 600 m)
5-First break picking	18-Post-stack time migration
6-Amplitude recovery	19-Pre-stack time migration
7-Ground roll noise attenuation	20-Post-stack FK3D
8-Wild amplitude noise attenuation	21-Post-stack random noise attenuation
9-Surface consistent amplitude compensation	22-Time-variant (TV) filter
10-Surface consistent deconvolution (operator length: 200 ms, gap: 16 ms)	23-Scale
12-Refraction statics correction	
13-1st pass velocity analysis (every 1200 m)/residual statics	

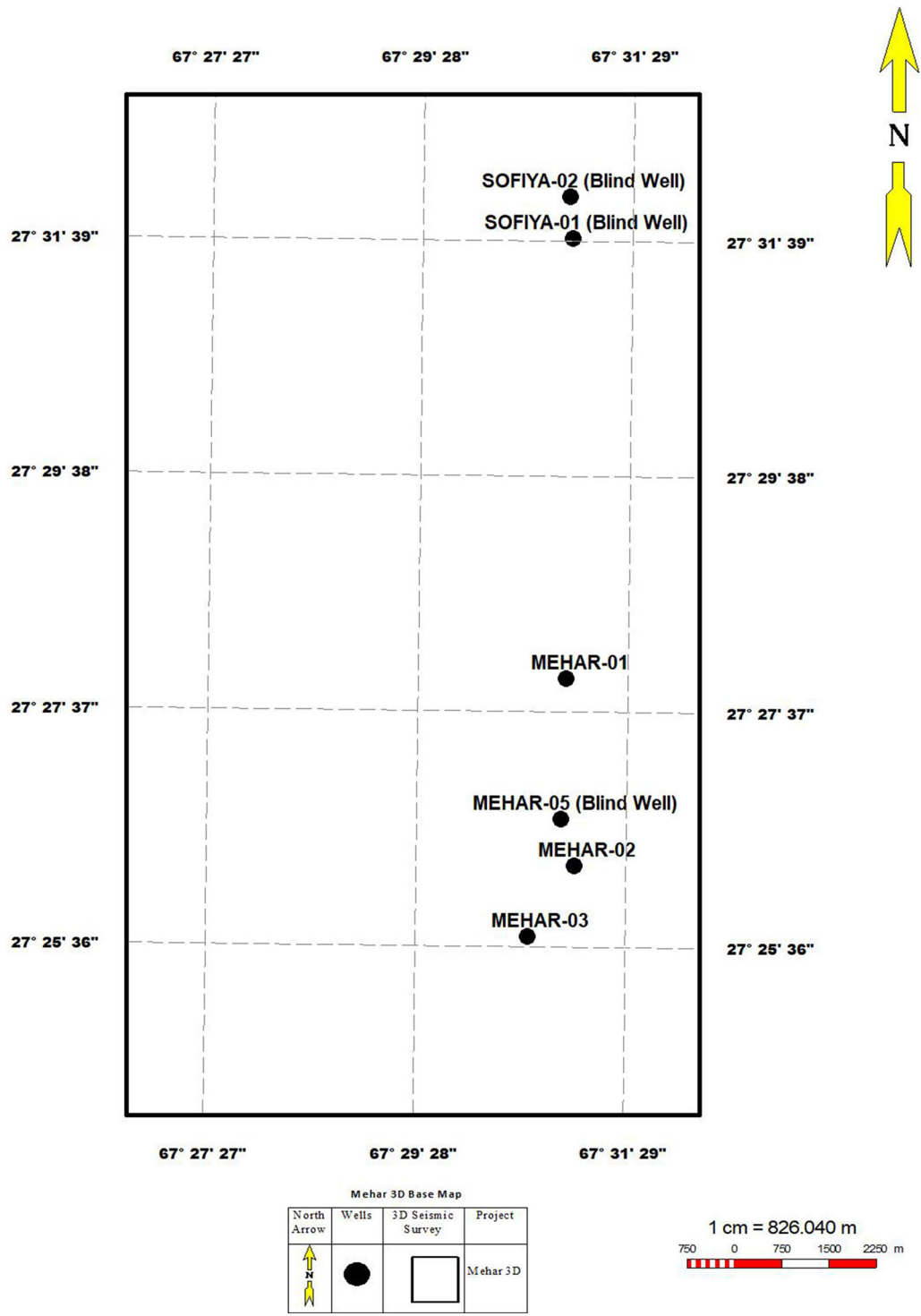


Figure 3

Base map of the 3D seismic cube showing its extent and well locations. The Mehar-01, Mehar-02, and Mehar-03 wells were used for analysis, while Mehar-05, Sofiya-01, and Sofiya-02 are the blind wells used for validation purposes

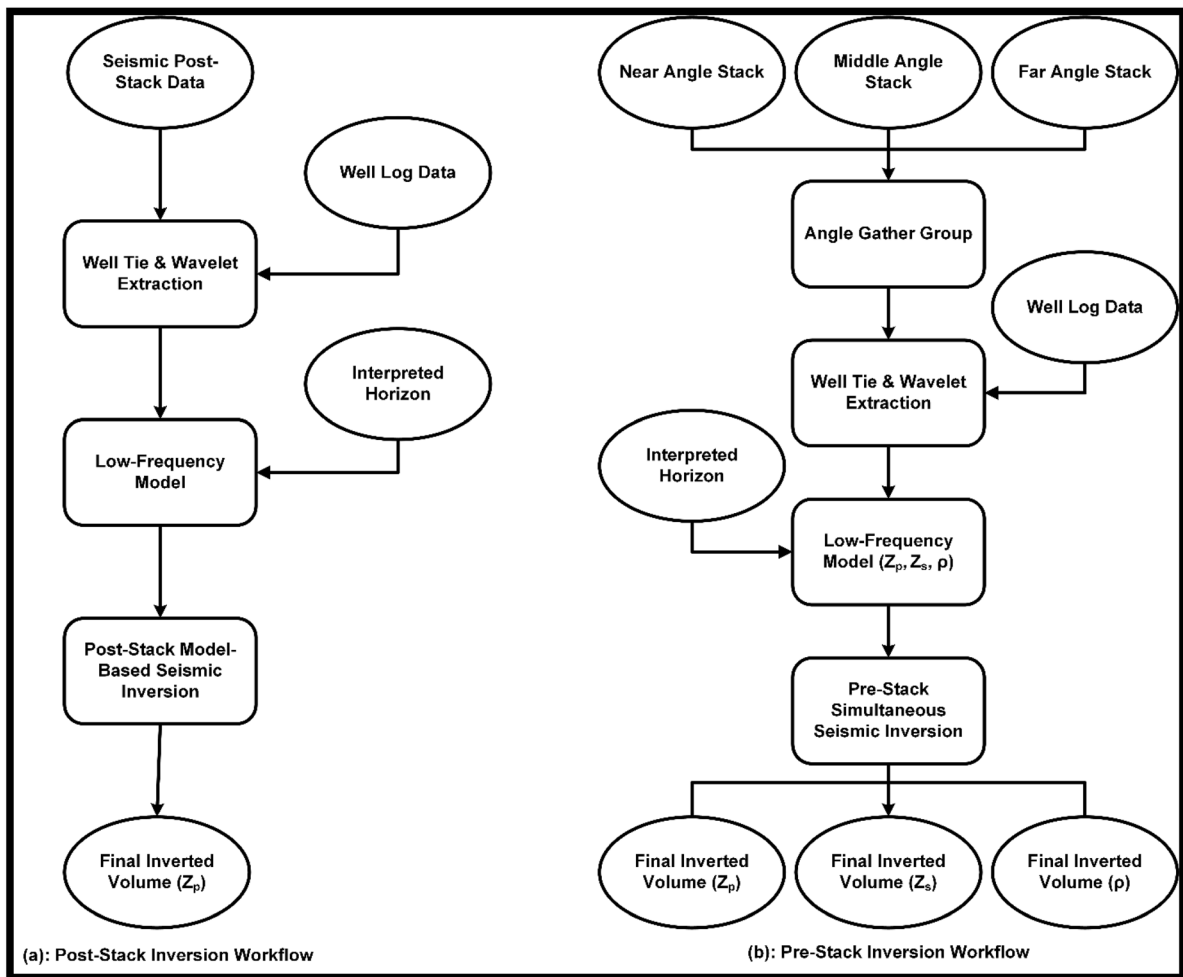


Figure 4

Workflow of seismic inversion, **a** Post-stack seismic inversion, **b** Pre-stack seismic inversion

4. Results

4.1. Seismic Interpretation

Proper understanding of subsurface configurations plays a dynamic role to accurately delineate the stratigraphic and structural traps (Emujakporue & Ngwueke, 2013). A thrust anticline with five horizons (Sui Main Limestone (SML), Ranikot, Lower Ranikot, Pab sandstone, and Mughalkot) and three thrust faults (Fault-01, Fault-02, and Fault-03) were marked on the seismic data. Fault-01 is the main fault that starts from the Cretaceous and cuts the whole Paleocene and Eocene sections (strata). The interpreted in-line (IL-591) shown in Fig. 5 indicates

that the eastern side of Fault-01 is under the influence of tectonic stresses as the seismic reflections are chaotic here, whereas, the western side looks very stable, and seismic reflectors are continuous and can be easily traced. Moreover, the amount of displacement along Fault-02 and 03 is minor.

4.2. Petrophysics

Petrophysics provides insight for estimating the physical properties of rocks, mainly the reservoir rock (Asquith et al., 2004; Ogilvie, 2006). In this study, detailed log analysis is carried out to predict the reservoir characteristics utilizing the workflow

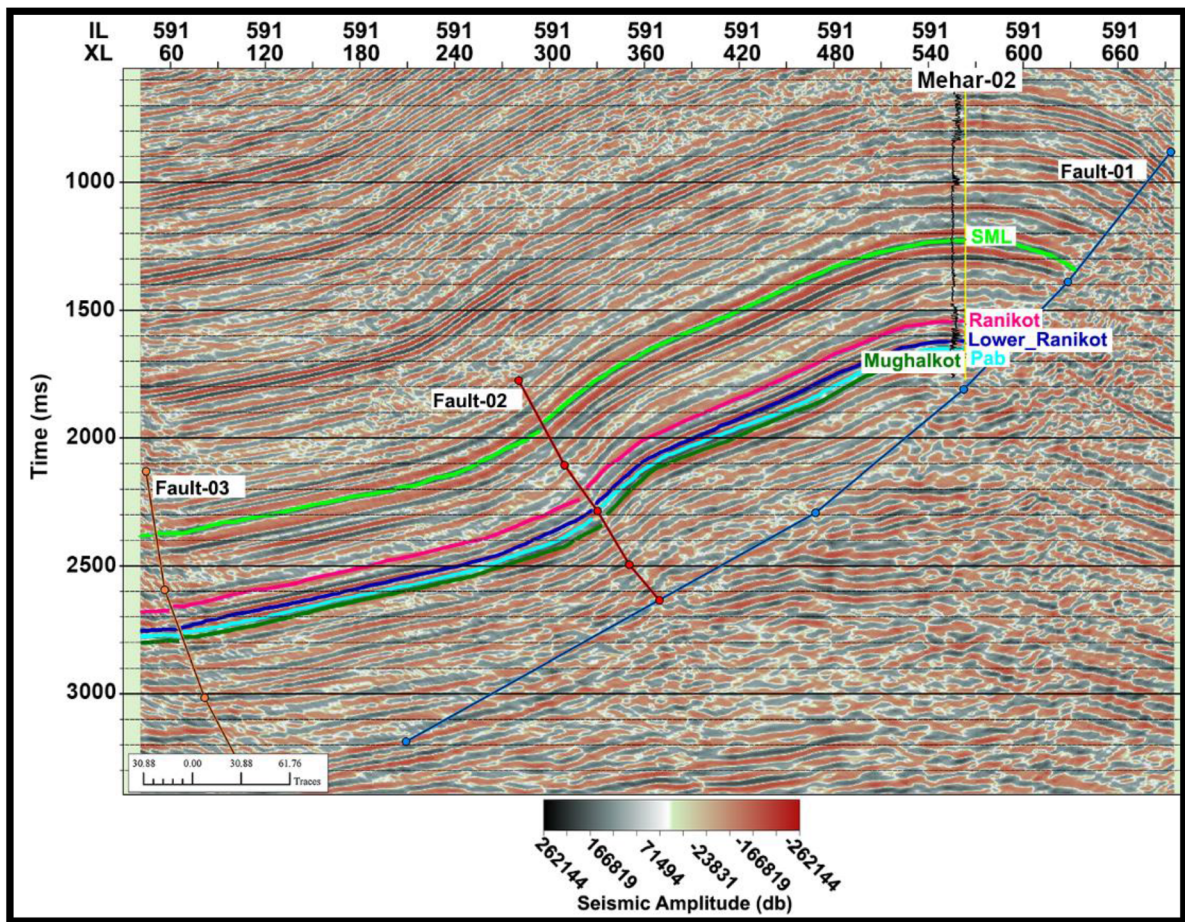


Figure 5

Seismic in-line IL-591 with different marked horizons and faults showing subsurface structural trends at the Mehar-02 well. Well-to-seismic tie was performed using vertical seismic profiling data of the Mehar-02 well. The marked horizons are shown with their respective colors

presented by Akhter et al., (2015) and Ali et al., (2018). More explicitly, the demarcation of clean zones, estimation of petrophysical properties, and net payable thicknesses were calculated based on the criteria/formulae defined by the aforesaid authors.

Based on the petrophysical analysis, it was observed that the upper part of the Ranikot Formation is not favorable for hydrocarbon production as it exhibits a high volume of shale, low effective porosity, high water saturation, low resistivity, and false crossover between neutron porosity and density logs, whereas, in the lower part, three hydrocarbon-bearing zones were identified as shown in Fig. 6. The thicknesses of zones 1, 2, and 3 are 4 m, 6 m, and 22 m, respectively. In zone 1, the observed average

values of volume of shale, effective porosity, and water saturation are 22%, 7%, and 21%, respectively. Zone 2 exhibits an almost similar value for volume of shale; however, in this zone, a considerable increase in effective porosity (11%) and decrease in water saturation (13%) was observed. Zone 3, having a fairly large thickness, shows more promising results as it exhibits a very low volume of shale (17%), high effective porosity (15%), and low water saturation (17%). The quantitative values of reservoir properties are presented in Table 2. All three zones have a low thickness and it is not possible to identify zones 1 and 2 on a seismic data set, so zone 3 was selected for further analysis.

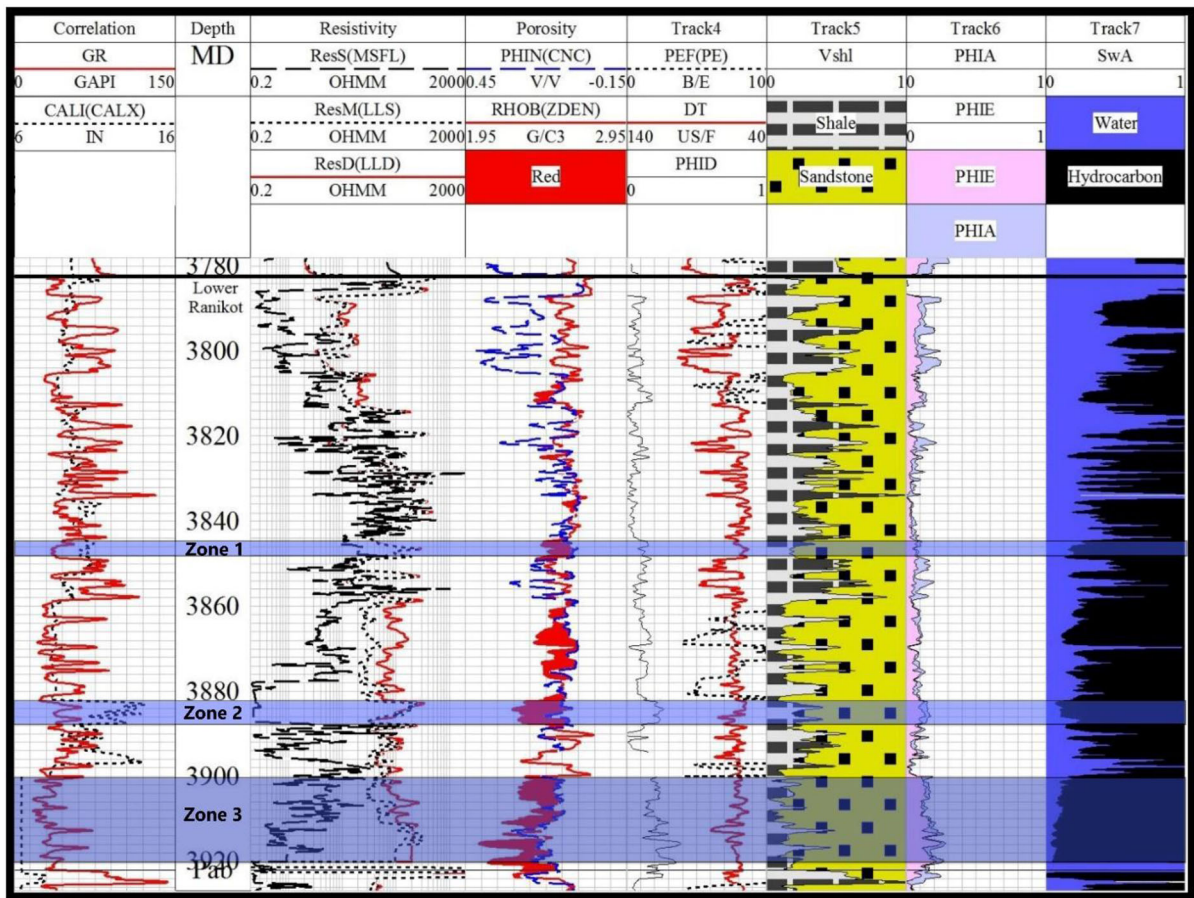


Figure 6

Well log interpretation of the Mehar-02 well with three marked zones of interest in the Lower Ranikot Formation. The last three columns represent the petrophysical properties calculated after analysis. In the last column the black and blue colors represent the hydrocarbon and water saturations, respectively. Yellow and grey in the third-to-last column indicate the lithological composition at various depths

Table 2

Zones of interest after petrophysical interpretation for Lower Ranikot in the Mehar-02 well

Lower Ranikot	Starting depth	Ending depth	Volume of shale (Vsh %)	Effective porosity (PHIE %)	Saturation of water (Sw %)	Saturation of hydrocarbon (Sh %)
Zone 1	3845	3849	21.67	6.73	20.61	73.39
Zone 2	3882	3888	25.53	11.01	13.62	86.38
Zone 3	3900	3922	16.64	14.89	16.95	83.05

4.3. Seismic Inversion

4.3.1 Seismic-to-Well Tie and Wavelet Extraction

Reflectivity series was generated using density and sonic logs. As seismic data are zero phase for this study, a statistical wavelet (zero phase) was extracted

initially for the well tie (Fig. 7), which was then convolved with the reflectivity series to get the synthetic traces. These synthetic traces were correlated with the seismic traces to attain the relationship between time and depth domains, and an initial well tie was established. Calibration of the three analyzed

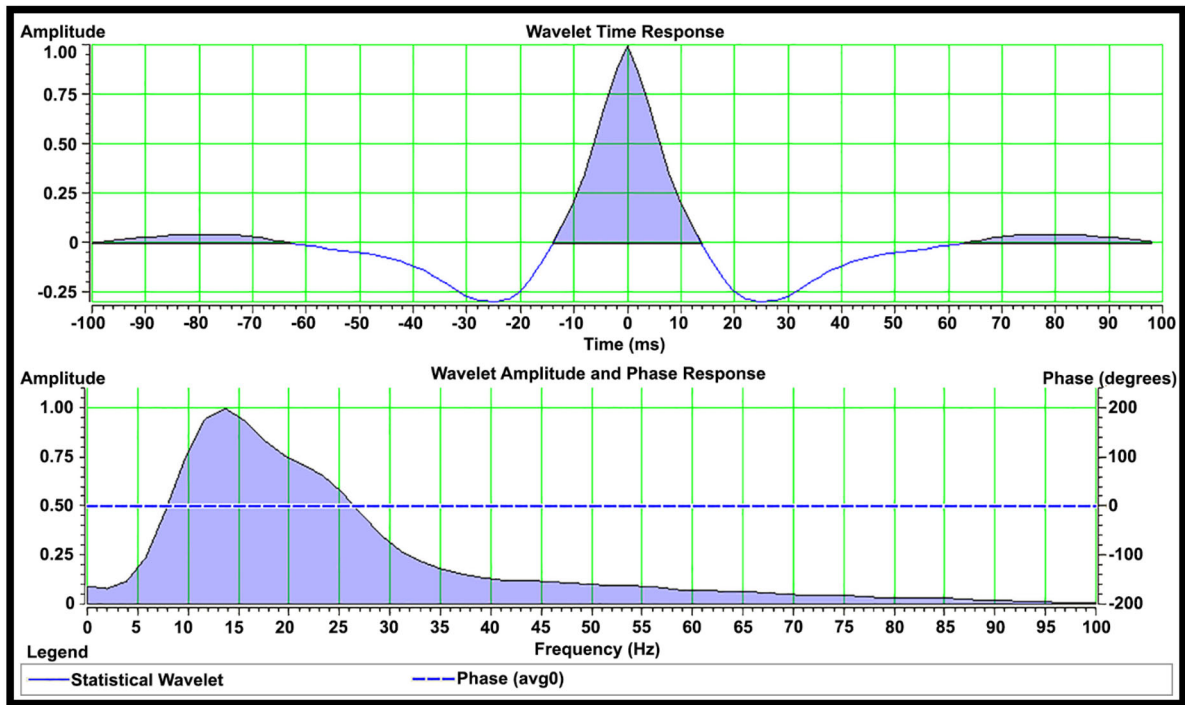


Figure 7

Extracted wavelet with phase and amplitude spectrum. Statistically computed wavelet extracted for each 10° incident angle. The wavelet has a broader frequency spectrum, providing detailed information on the subsurface. The wavelength of the wavelet is 200 ms, usually kept as $1/3$ of the inversion window. The dotted line displays the zero-phase average amplitude of the wavelet

wells was performed by using available refined check shot data; consequently, a significant time shift by stretching and squeezing the synthetic traces was not applied to achieve a good correlation here. Further, a well-based wavelet was extracted to maximize the correlation between synthetic and seismic traces.

The size of the cross-correlation plot is set up to the largest possible time window having both synthetic and real traces. The start time is 1200 ms, which ended at 1750 ms, enclosed by the two yellow lines to demarcate the correlation zone (Fig. 8). An excellent correlation coefficient of 84% is achieved between synthetic and seismic traces, with a more symmetrical shape around the zero-lag time.

4.3.2 Low-Frequency Model (LFM)

Seismic data are generally missing in low frequencies, so to incorporate them, LFM is generated using a low-pass filter. A low-pass filter allows low

frequencies up to 10 Hz to pass and filters out frequencies above 15 Hz. For LFM generation, only the Z_p log was utilized in PMBSI, while Z_p , Z_s and density logs from each well were used in PSSI. These extracted logs were interpolated between the wells and along the horizons using a triangular interpolation technique. The obtained model shows evident lateral and vertical impedance variations within the zone of interest. The lateral variations show the extent of different facies, whereas the vertical one indicates the change in lithology (Fig. 9).

4.3.3 Post-Stack Model-Based Seismic Inversion (PMBSI)

PMBSI effectively highlights the lateral and vertical geometrical variations in Z_p using a low-frequency model (Ali et al., 2018). PMBSI is based on the convolution model, which can be expressed from a

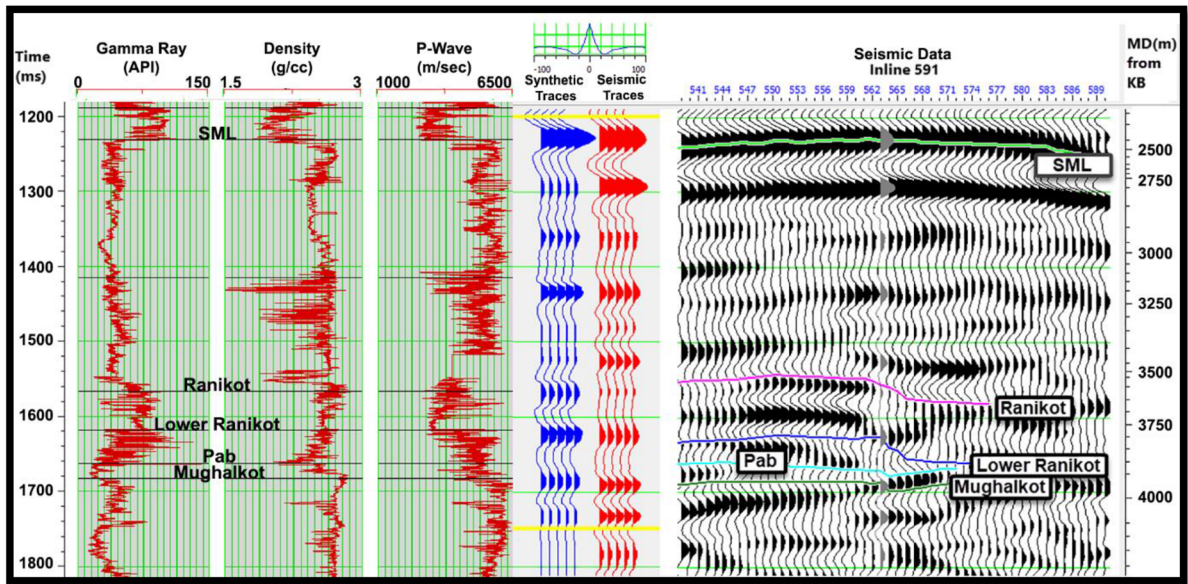


Figure 8

Seismic-to-well correlation with the Mehar-02 well. The blue traces are synthetic traces calculated from the sonic and density logs, in this well with the extracted wavelet in fourth track. The red traces are the average or composite traces extracted from the seismic data. The correlation window start and end time was kept from 1200 to 1750 ms, respectively, highlighted by the two yellow lines. In the seismic data column, a highlighted trace is a field trace along the well

non-linear and band-limited equation (Swisi, 2009) as follows.

$$S_t = W_t * R_t + N_t, \quad (1)$$

where S_t is the seismic trace, W_t is the seismic wavelet, R_t is the reflectivity in the time domain, $*$ represents convolution operator and N_t is the noise component. PMBSI reduces the recursive inverse problems through an iterative manner by providing least-square best fit reflectivity to seismic data (Hampson et al., 2005; Lee et al., 2013). The equation used for the PMBSI explained by Hampson et al., (2005) is given in Eq. (2).

$$J = Weight_1 \times (S_t - W_t * R_t) + Weight_2 \times (M - H * R_t), \quad (2)$$

where J is the objective function and M reflects the initial guess impedance model, which can be derived from well logs, and H is the integration operator, which can be convolved with the reflectivity to obtain the acoustic impedance.

In PMBSI, an a priori impedance model was convolved with the best-fit wavelet to get a synthetic trace comparable to the actual seismic trace. The impedance model was iteratively altered to reduce the error and get optimal matching up to the threshold value. The threshold values in Eq. (2) were actual weights ($Weight_1$ and $Weight_2$), and the model with minimum errors provides the solution.

In Eq. (2), minimizing the first part provides the solution to model the seismic trace, while minimizing the second part provides the solution for priori impedance defining the specified block size. These conditions are usually incompatible, so the weight values determine how this was balanced. In constrained model-based inversion, $Weight_2$ is 0, and the final impedance values were customized within upper and lower bounds (maximum impedance change). In this study, inversion was run using hard constraint, so the output model cannot go beyond these values. The PMBSI algorithm was selected, because it allows the impedance model to update iteratively by improving the best correlation between actual and synthetic traces. PMBSI parameters were optimized

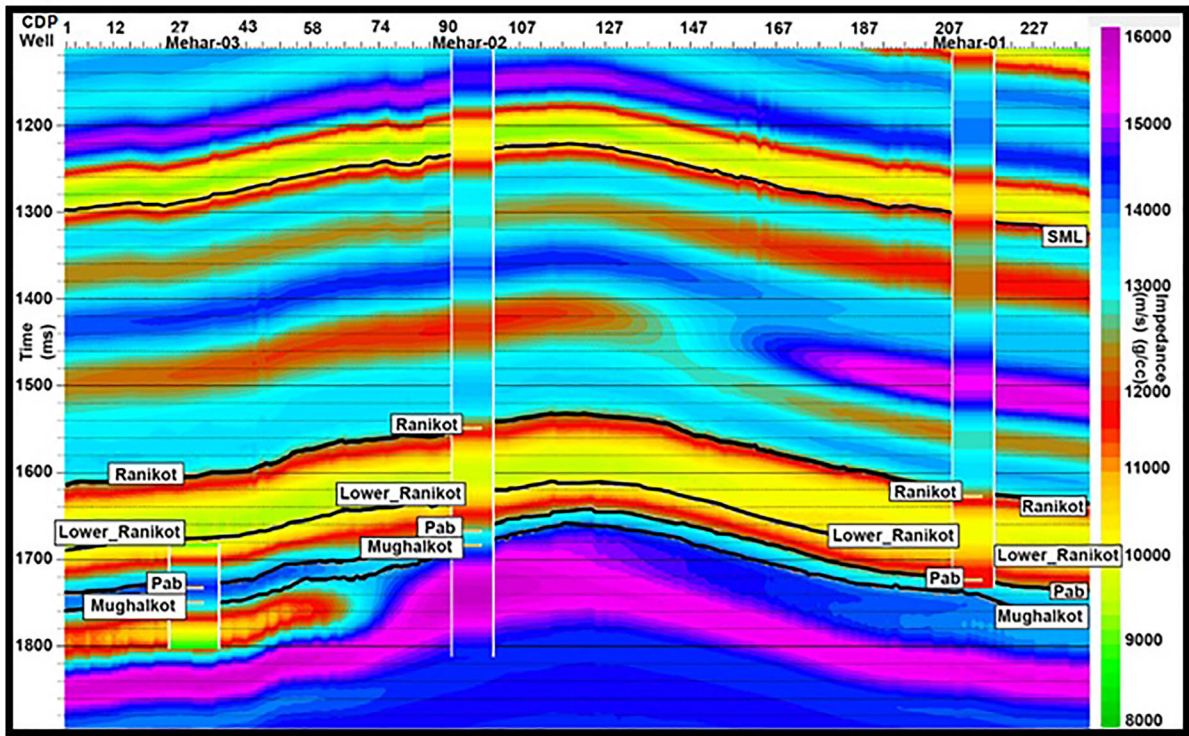


Figure 9

Arbitrary line passing through the wells showing the low-frequency model used for post- and pre-stack inversion study overlain by the wells

using the inversion analysis process and later verified at the well locations.

Meanwhile, scalars automatically scale the input seismic data to the amplitude range of the synthetic seismic data. The method is applied by keeping hard constraint limits up to 100% for lower/upper limits with pre-whitening up to 1% and average block size to 2 ms. Full spectrum seismic inversion is chosen for the output results by keeping 20 iterations.

PMBSI performed at the reservoir level (Lower Ranikot) depicted low values of Z_p , ranging from 8000 to 9000 (m/s)(g/cc), embedded between comparatively high impedance values, ranging from 9500 to 11,000 (m/s)(g/cc). Low Z_p values indicate payable zones (gas sands), and high values indicate the non-payable zones. Well logs and inversion results show reasonable matching of impedances at the desired depth, which indicates the reliability of inversion results (Fig. 10). Moreover, a post-stack arithmetic mean impedance (Z_p) map, considering 30 ms thickness from the top of the interpreted

horizon, was generated, which confirmed the presence of producing wells in the low Z_p zone. The inverted results were further validated through the blind wells (Sofiya-01, 02 and Mehar-05) lying in the same low impedance zone (Fig. 11). The applied PMBSI provided good calibration with the log curves regarding low impedances, but it was unable to resolve thin sand beds (4–22 m) of the Lower Ranikot Formation demarcated by petrophysical analysis. Therefore, a feasibility study was carried out by cross-plotting petrophysical and elastic properties to select the suitable inversion algorithm which could accurately resolve the thin beds of the Lower Ranikot Formation.

4.3.4 Cross-Plot Analysis

Elastic attributes are commonly used to demarcate different types of facies. However, the separation of hydrocarbon- and non-hydrocarbon-bearing zones sometimes becomes difficult based on a single

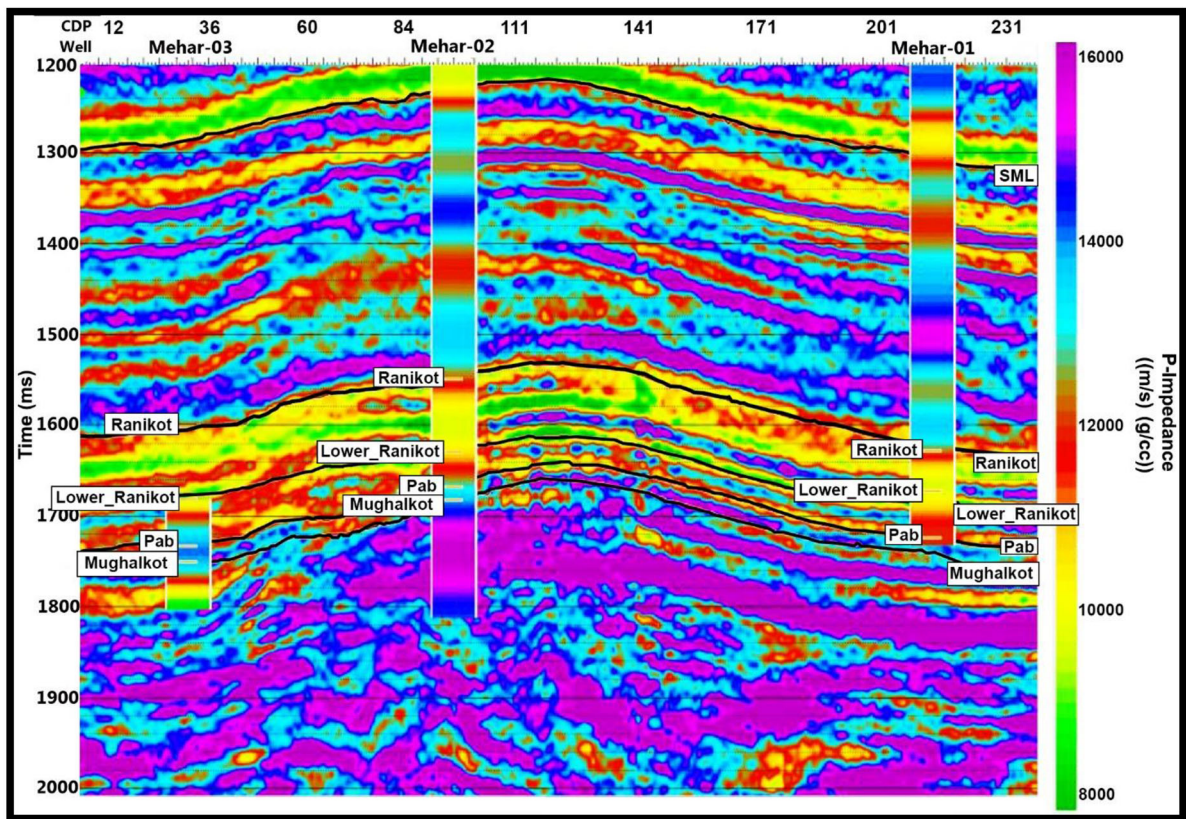


Figure 10

Arbitrary line of inverted post-stack Z_p volume passing through the wells (Mehar-01, 02, and 03) with overlaid Z_p logs. The well impedances are matching with the inverted Z_p validating the results

attribute (Odegaard and Avseth, 2004; Hughes et al., 2008; Chi & Han, 2009) such as in the study area. The cross-plots with a combination of different elastic and petrophysical attributes differentiate the gas-bearing and non-gas-bearing sediments (Fig. 12a–c). These cross-plots were generated utilizing Z_p on the x-axis and V_p/V_s on the y-axis by keeping the important petrophysical properties (volume of shale (Fig. 12a), effective porosity (Fig. 12b) and water saturation (Fig. 12c)) as a color code (z-axis). To be a productive gas zone, the volume of shale should be low, effective porosity should be relatively high and water saturation should be low. Cross-plots indicate that pay gas sand cannot be separated based on a single elastic property (Z_p) which means PMBSI was not the solution to characterize this reservoir. It can be separated by combining Z_p and V_p/V_s attributes. The cross-plots

presented in Fig. 12a–c complement each other and demarcate the gas-bearing zone more efficiently. Therefore, pre-stack simultaneous inversion was performed to characterize this reservoir.

4.3.5 Pre-Stack Simultaneous Seismic Inversion (PSSI)

PSSI has the principal advantage over two-step PMBSI as it provides a variety of information that can be utilized to separate potential zones from non-potential zones. In pre-stack inversion, data is angle-dependent resulting in that Z_p and Z_s along with the V_p/V_s ratio and can be utilized effectively to solve complex scenarios, which were not possible with post-stack inversion (Hampson et al., 2005; Sams & Carter, 2017). Therefore, simultaneous inversion was applied to couple the effects between the variables,

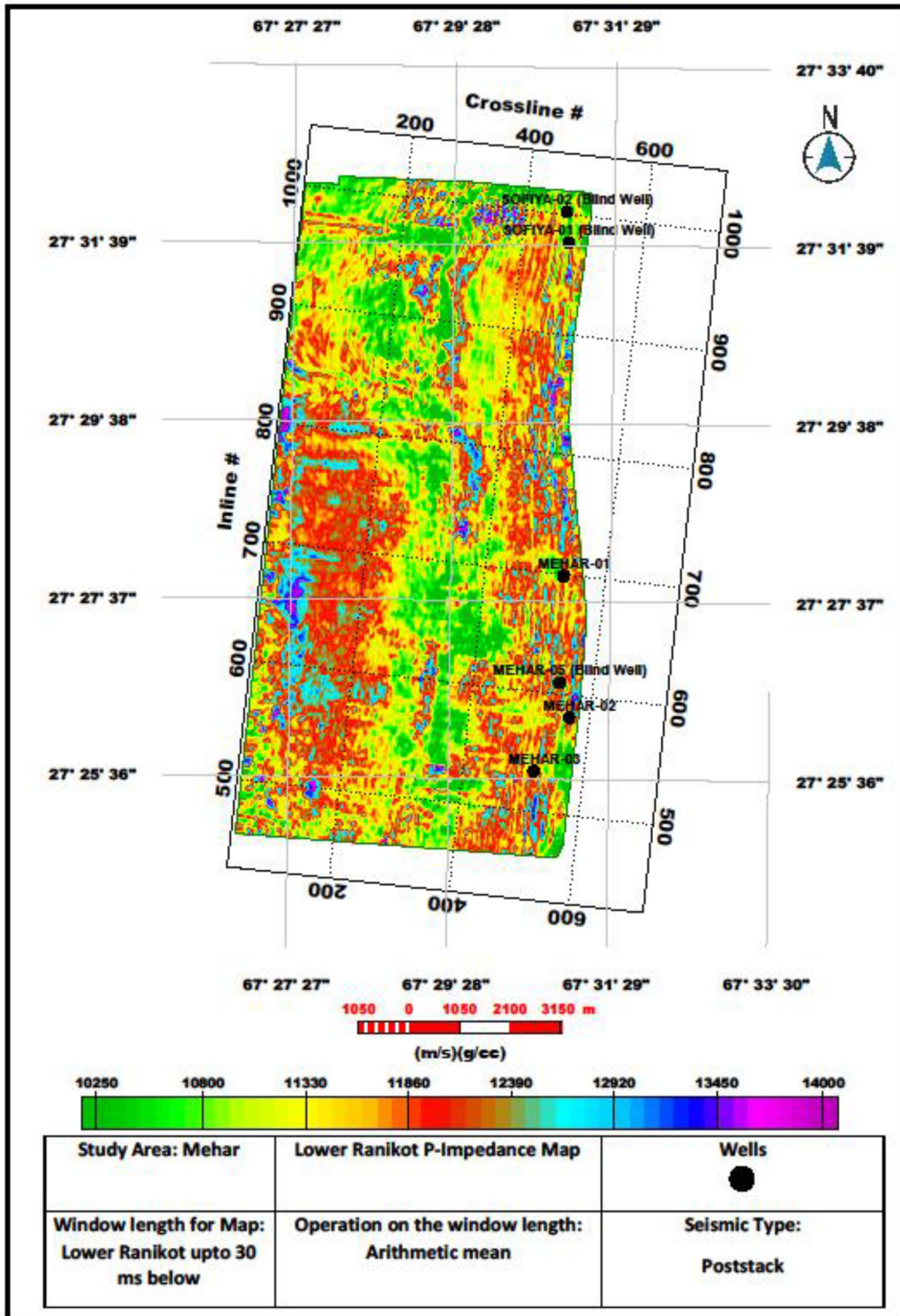


Figure 11 Arithmetic mean of Z_p using PMBSI at Lower Ranikot, with a window of 30 ms below the interpreted horizon

which were sensitive to noise and usually produce non-unique solutions. The modified Fatti's equation is utilized in this study for the application of PSSI, as the effects of the attenuation due to larger offsets can be handled very well due to angle dependence of the extracted wavelet (Fatti et al., 1994; Hampson et al., 2005; Russell & Hampson, 1991) given as.

$$T(\theta) = \left(\frac{1}{2}\right)c_1W(\theta)DL_p + \left(\frac{1}{2}\right)c_2W(\theta)DL_s + \left(\frac{1}{2}\right)c_3W(\theta)DL_d. \quad (3)$$

Here, $T(\theta)$ is the seismic trace at angle θ , $W(\theta)$ is the wavelet at angle θ and D is the derivative operator where $L_p=\ln(Z_p)$, $L_s=\ln(Z_s)$, and $L_d=\ln(\rho)$, are the natural logarithms of Z_p , Z_s , and ρ , respectively. c_1 , c_2 , and c_3 are constant components defined by

$c_1 = 1 + \tan^2\theta$, $c_2 = -8\gamma^2\tan^2\theta$, $c_3 = -0.5\tan^2\theta + 2\gamma^2\sin^2\theta$, and $\gamma = V_s/V_p$ (Aki & Richards, 1989; Zoepritz, 1919; Hampson et al., 2005).

For the background ratio V_s/V_p , i.e., γ , a value of 0.5 is applied here for wet sands and shales, and it worked best. For pre-whitening, the % pre-whitening method was used to supply individual pre-whitening values for each parameter. These values were calculated to be 1, 0.01, and 0.01 for Z_p , Z_s , and ρ , respectively. Finally, inversion was successfully applied with 20 iterations.

To ensure the validity of the inversion results, several quality checks have been performed. Figure 13 shows the comparisons of the well impedance (synthetic in blue) and the final inverted Z_p (red) at the location of the Mehar-02 well. A filter of 8–12 Hz was applied on well data to adjust the frequencies of seismic and well data sets. A minimum of 20 iterations have been applied to minimize the error between the synthetic and inverted curves. The comparison in Fig. 13 shows a maximum value of correlation coefficient = 92.87% with minimum error.

The output of pre-stack inversion was represented as inverted Z_p , Z_s , and V_p/V_s ratio volumes (Figs. 14, 15, 16). Calibration of inverted results with well log data showed very good matching within the zone of interest (Lower Ranikot) at the well locations. Low impedance (in green) resides between high impedance (in red) at the reservoir level (time window around 1600 ms), which is fairly well-linked

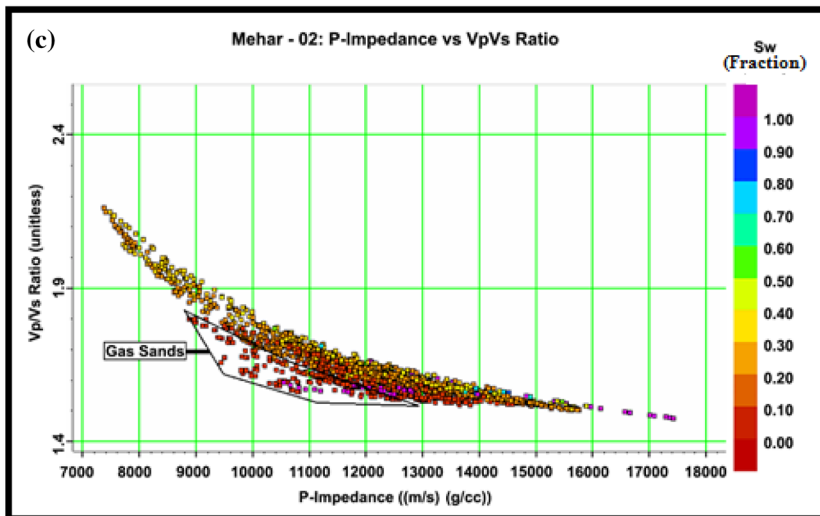
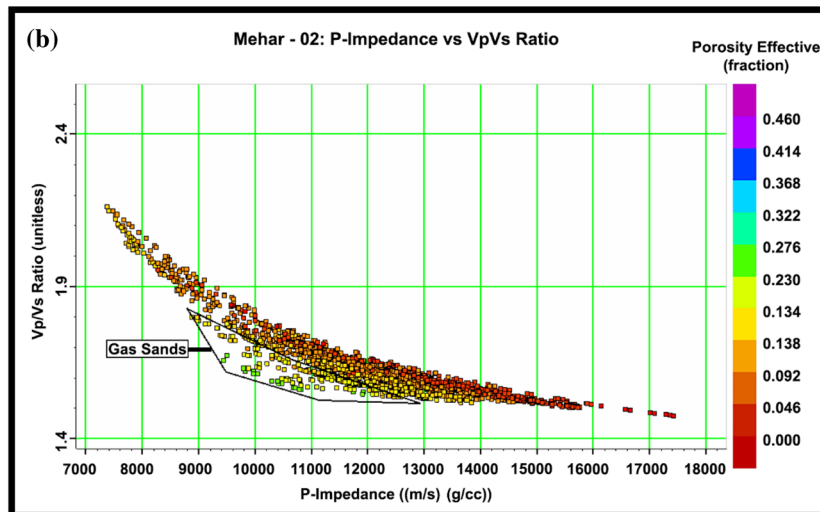
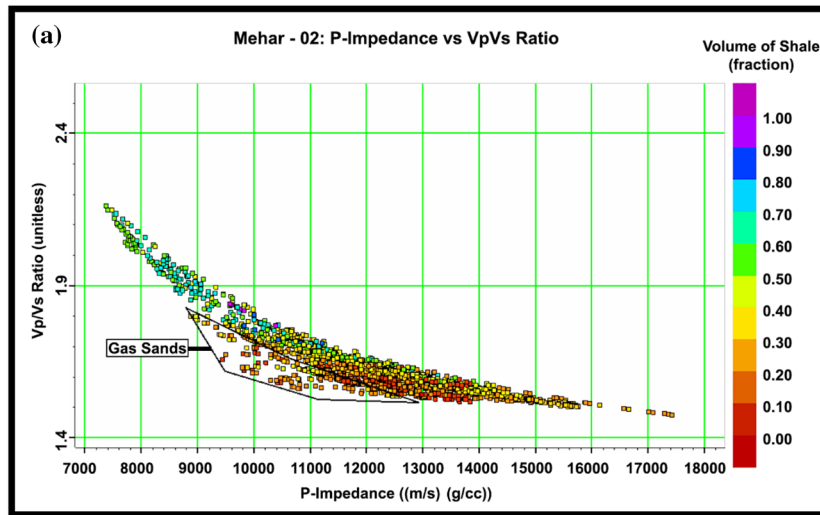
with the amount of fluid content present in that particular zone. In Fig. 14, the low Z_p values ranges from 8000 to 9333 (m/s)(g/cc), with high Z_p gaining a value up to 11,500 (m/s)(g/cc). Further, the inverted Z_s attribute also replicated the results obtained from Z_p with low Z_s values ranging from 5000 to 6000 (m/s)(g/cc) bounded between relatively higher Z_s ranging from 7000 to 8000 (m/s)(g/cc) (Fig. 15).

The most reliable and sensitive attribute extracted in pre-stack inversion is V_p/V_s , which has pivotal role in distinctly highlighting the sweet spots. As the presence of hydrocarbon drastically decreases the compressional wave velocity (V_p) by relatively increasing the shear wave (V_s) component, so the ratio of V_p/V_s turns out to be more sensitive to analyze the amount and change of fluid type as compared to V_p or V_s separately. Generally, the V_p/V_s ratio ranges up to 1.6 in gas sands so a similar range of about 1.65 is observed at the Lower Ranikot level. Thus, the three inverted PSSI attributes successfully delineated the gas prone thin sand packages at the targeted reservoir zone.

Furthermore, mean arithmetic Z_p , Z_s and V_p/V_s ratio maps extracted within a time window of 30 ms from the top of the Lower Ranikot on seismic cube also provided strong evidence of gas presence (Figs. 17, 18, 19). The arithmetic mean maps for the three attributes showed the anomalous zone at the three utilized wells, and a similar anomalous behavior was depicted at the blind well locations further validating the PSSI results.

4.3.6 Porosity Prediction

Porosity is the available volume of space that fluids can occupy (Nimmo, 2004). Accurate estimation of porosity at and away from the well is the most critical step. It plays a vital role for tight sand reservoirs to produce oil and gas economically, as in this study. The porosity derivation from impedance is based on the empirical relation established between actual and predicted porosities using PMBSI and PSSI attributes at the well locations, which in turn was used to extrapolate over the entire seismic volume (Helgesen et al., 2000; Çemen et al., 2014; Busch et al., 2019). Generally, linear and multi-linear regression analyses are adopted to develop a relation between



◀Figure 12

a-c Feasibility study cross-plots of petrophysical and elastic attributes at the Mehar-02 well. 12a: P-Impedance (Z_p) vs. V_p/V_s with the color bar representing volume of shale variations in volume fractions. 12b: P-Impedance (Z_p) vs. V_p/V_s with the color bar representing effective porosity variations in volume fractions. 12c: P-Impedance (Z_p) vs. V_p/V_s with the color bar representing water saturation variations in volume fractions

petrophysical and elastic properties (Hampson et al., 2001; Lorenzen, 2018). The efficacy of multi-linear regression has some limitations due to strong variability in the reservoir properties, so artificial neural network techniques such as PNN are suggested, which are able to handle complex problems without having prior knowledge of the process (Durrani et al., 2020).

PNN is a mathematical interpolation technique, which estimates a non-linear relation by training the petrophysical input logs (effective porosity and volume of shale) with internal (sample-based seismic volume) and external attributes (impedances and V_p/V_s ratio) at well locations (Liu & Liu, 1998; Sinaga et al., 2019). The non-linearity enhances the predictive power as it breaks the input data into parts called feature extraction. The internal attributes were calculated by mathematical transformation of multiple post-stack seismic attributes including trace

envelope, amplitude-weighted cosine phase, and instantaneous phase, while external attributes calculation was performed on inverted seismic elastic attributes (Dorrington & Link, 2004). This procedure reduces the dimensionality of the data before they are applied to train the system.

PNN was applied here to enhance the resolution and to predict the porosity over the impedance volume. Three wells have been used to train the calculated seismic attributes. The correlation coefficient achieved in the cross plot (Fig. 20) via the regression technique showed a fairly good match (95% correlation) between actual and predicted porosities. Inverted porosity sections showed a strong correlation with well log computed porosity curves. The relative increase of porosity embedded in low impedance sand zones justifies the gas presence. The calculated average porosity of thin sand zones of the Lower Ranikot Formation through petrophysical analysis is 11% (Fig. 6). The inverted porosities in low impedance zones range from 11 to 13% (Figs. 21, 22). A good match between well and inverted porosities calculated at the three well locations raised the confidence level for the applied technique.

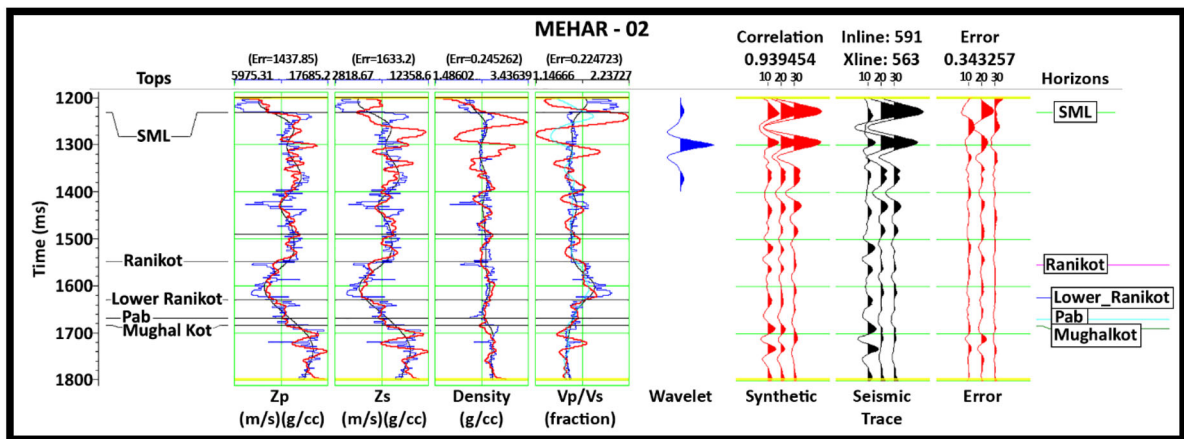


Figure 13

Pre-stack inversion error analysis at the Mehar-02 well. The display shows the inversion result (red curve), original impedance log from the well (blue curve), an initial model (black curve) for all the tracks, including Z_p , Z_s , density and V_p/V_s ratio. Blue is the selected wavelet in the wavelet track; synthetic traces are shown in red followed by the original seismic composite trace in black. Finally, the error trace, which is the difference between the two previous results showing a minimum value is presented

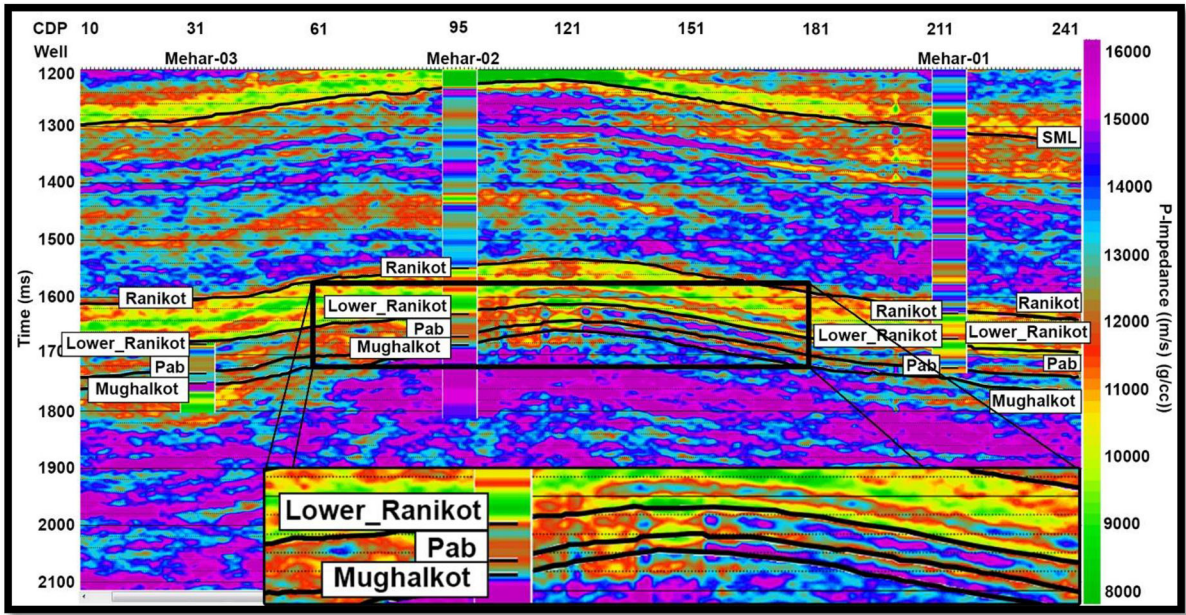


Figure 14

Arbitrary line of PSSI Z_p volume passing through the wells (Mehar-01, 02, and 03) with overlaid Z_p logs. The zone around Mehar-02 is zoomed in to highlight the important characteristics

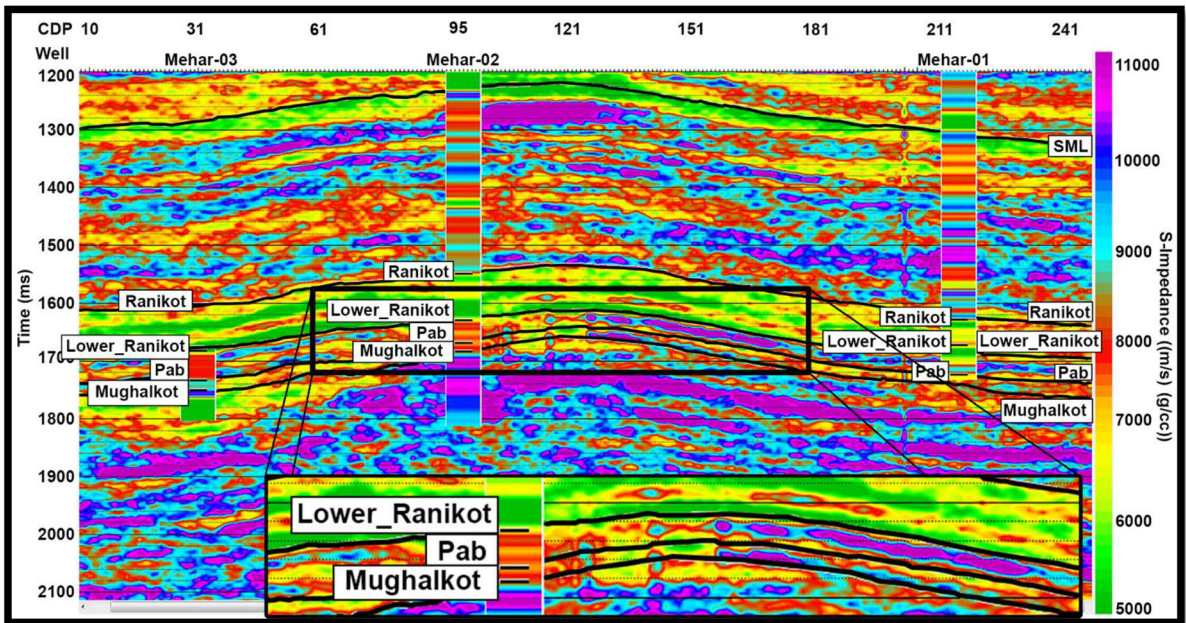


Figure 15

Arbitrary line of PSSI Z_s volume passing through the wells (Mehar-01, 02, and 03) with overlaid Z_s logs. The zone around Mehar-02 is zoomed in to highlight the important characteristics

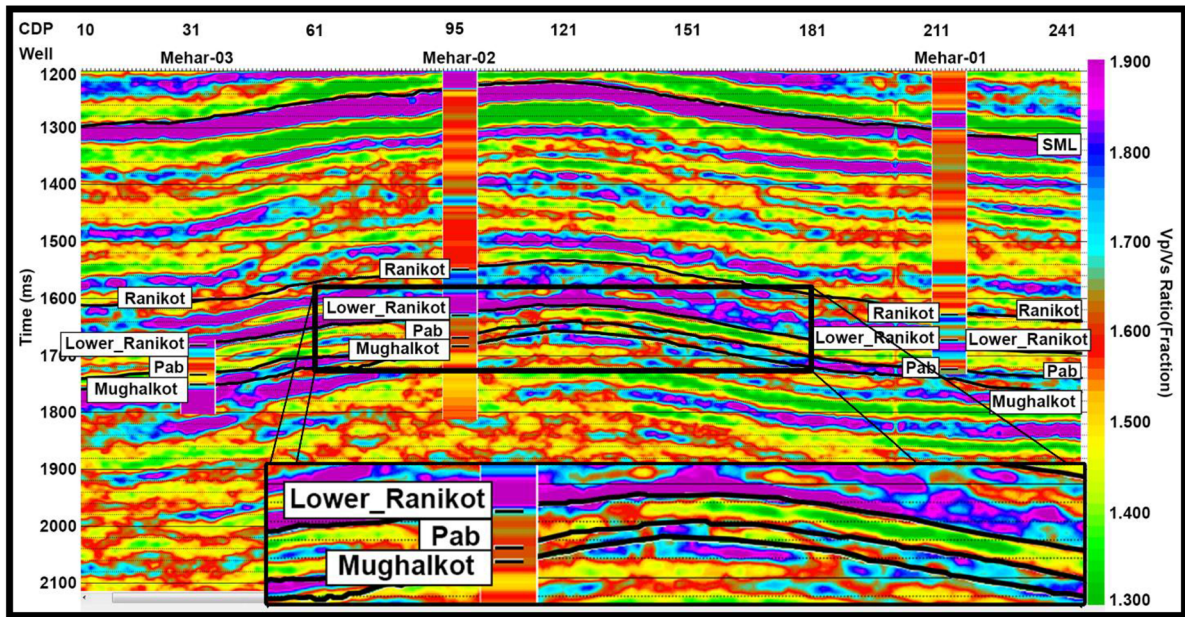


Figure 16

Arbitrary line of PSSI Vp/Vs volume passing through the wells (Mehar-01, 02, and 03) with overlaid Vp/Vs logs. The zone around Mehar-02 is zoomed in to highlight the important characteristics

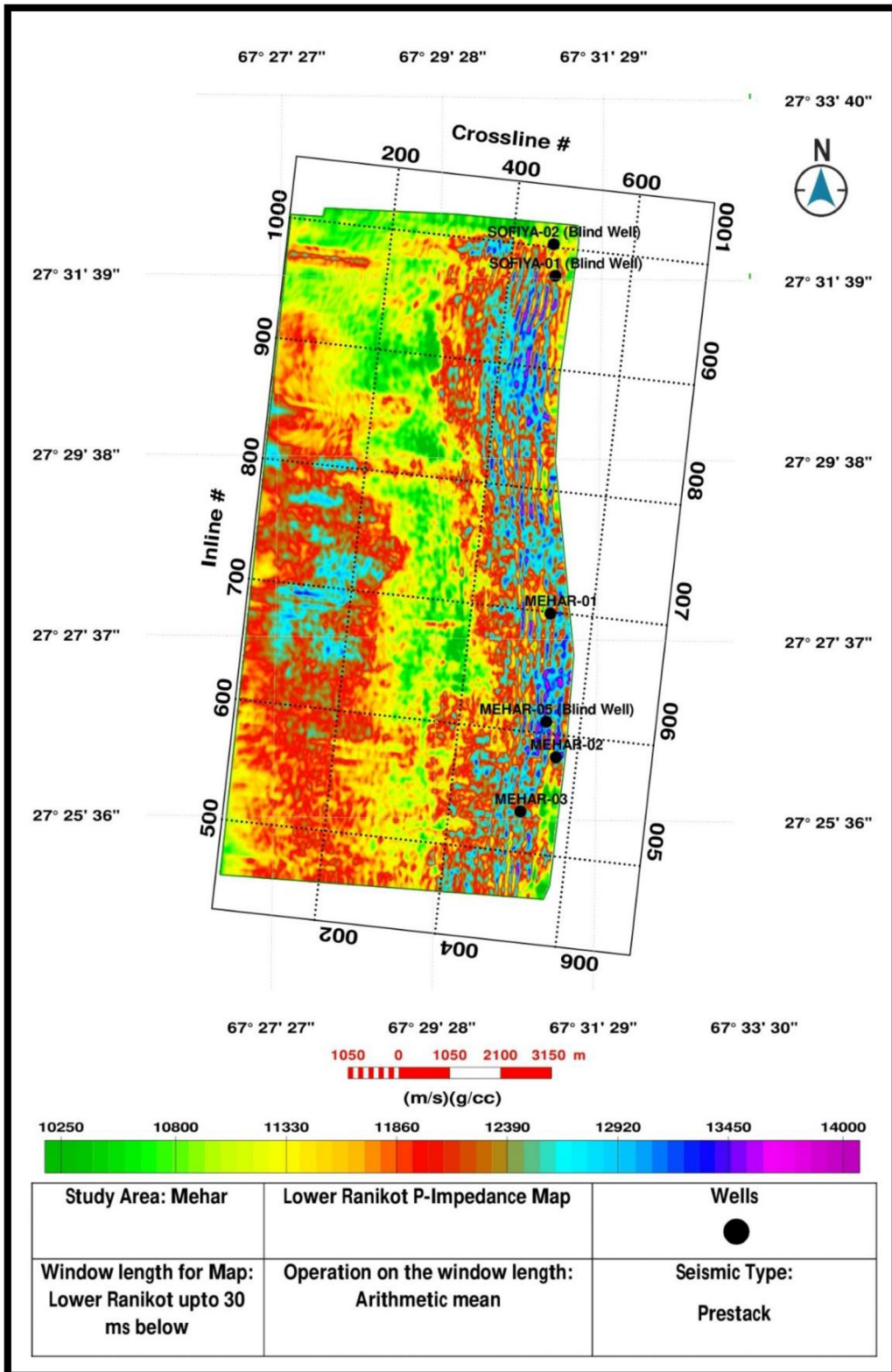
5. Discussion

Formulating a technique for evaluating the untapped and heterogeneous reservoirs using the seismic inversion process is a challenging task. PSSI has been applied successfully in many basins with complex tectonics to quantify the lithology and fluid distribution (Lu et al., 2020; Moghanloo et al., 2018). The study performed by Young et al., (2016) using PSSI in the Malay basin effectively discriminated the lithology and demarcated the thin gas sand layer. Similarly, lithology and fluid prediction were also made possible using PSSI for the near shoreface sands of Agbada and Benin Formations in Sandfish field, Niger Delta, Nigeria (Adeoti et al., 2018). Further, gas potential in the sand-shale layer and porosity distribution of Tipam Sandstone of the Miocene age in the Upper Assam basin of India has also been highlighted by pre-stack inversion attributes (Gogoi & Chatterjee, 2019).

The gas-bearing sands of the Lower Ranikot Formation act as the main reservoir in the study area (Haider et al., 2012). Petrophysical analyses suggest

that Lower Ranikot sand contains three hydrocarbon-bearing zones with thickness ranging from 4 to 22 m (Fig. 6). The spatial distribution of these zones was analyzed through seismic inversion. Seismic inversion has been proved to be the best interpretation method to decipher the subsurface geometries, especially when complex reservoirs demand quantification of the reservoir characteristics in terms of porosity, lithology, and fluid content (Anna et al., 2009; Zoya and Carlos, 2013).

Firstly, PMBSI was performed, which provided satisfactory results by depicting low impedance hydrocarbon-bearing sands; however, it could not separate the thin sand and shale layers within the zone of interest (Fig. 10). Typically, PMBSI with Z_p as output is used to delineate the different types of lithology and payable zones (Miller & Stewart, 1990); however, in geologically complex reservoirs, Z_p alone is insufficient for accurate reservoir characterization (Huang & Liu, 2013). Therefore, to analyze the sensitivity of elastic parameters, both petrophysical and elastic parameters were cross-plotted, confirming that pay gas cannot be separated



◀Figure 17

Arithmetic mean of Z_p using PSSI at Lower Ranikot, with a window of 30 ms below the interpreted horizon

based on a single elastic parameter (Z_p) (Fig. 12a–c). This means an addition of shear wave information is crucial, which in combination with other parameters such as Z_p and V_p/V_s can solve the problems of porosity with accurate demarcation of reservoir boundaries (Li et al., 2013). PSSI provides a variety of inversion parameters that permit us to solve those problems which were not resolved by post-stack inversion.

Pre-stack inversion results depict that the Z_p attribute shows almost similar impedance variations as observed through post-stack inversion (Fig. 14). However, inverted Z_s and particularly V_p/V_s results provide more prolific and enhanced reservoir characterization as V_p/V_s attribute demarcate the top and bottom of the Lower Ranikot Formation (Fig. 16). Results of PSSI are validated with the well logs at the reservoir level, which shows that absolute values of inverted Z_p , Z_s , and V_p/V_s are in good agreement with the absolute values derived from well logs (Figs. 14, Fig. 15, Fig. 16). However, a bit high values of the Z_p attribute within the reservoir zone may be due to little strings of limestone. Overall, low impedance zones of the Lower Ranikot Formation are more prominent with relative appreciable thickness in the pre-stack inverted sections, especially in the V_p/V_s sections compared to the post-stack results.

The ultimate goal in reservoir characterization is to translate the elastic properties into reservoir properties. Porosity plays a vital role in quantifying the hydrocarbon potential of the reservoir. The inverted and predicted porosities are cross-plotted in order to analyze the correlation between them (Fig. 20). The values of inverted porosities for pay zones range from 11 to 13%, which agree with the well porosities (11%, Figs. 21–22). Valzania et al., (2011) and Berger et al., (2009) also suggested that porosity values of gas sands in the Lower Indus Basin lie between 8 and 12%, and these sands have a very high potential of producing hydrocarbons. From the

above analysis, it was also observed that an increase in porosity and decrease in Z_p values directly relates to the saturation of hydrocarbon and the thickness of the reservoir. The results of PSSI were also verified using three blind wells of the Mehar field. The current findings and their validation with blind wells represent good to excellent matching, which confirms the authenticity of our study. However, uncertainty is always present, which can be further minimized by integrating the available geological data.

The applied techniques will be helpful for delineating the heterogeneous thin hydrocarbon reservoirs in basins having similar geological and tectonic settings, such as Iran, India, Malay, Nigeria, and China. It will also boost the confidence level of geoscientists to drill in the fold and thrust belts.

6. Conclusions

Integrated analysis through post-stack and pre-stack seismic inversions and well log data has been successfully carried out for reservoir characterization of thin sands of the Lower Ranikot Formation, Pakistan. This formation is the primary target in the study area, which due to its variegated lithology and thickness, possesses a challenge to tap the hydrocarbon potential. Three prolific gas zones have been identified via well log analysis which bears very good correlation with seismic markers. The application of PMBSI highlights the low impedance zones as well as the geometry of the reservoir. However, the results of PSSI provide more accuracy, especially the V_p/V_s attribute effectively separated thin gas sand layers. As porosity is the navigating tool in delineating the sweet spots in gas reservoirs, it was predicted using PNN. An excellent correlation was found between inverted (11–13%) and actual porosities (10–12%), improving our confidence level for exploration of thin gas untapped pockets away from the well.

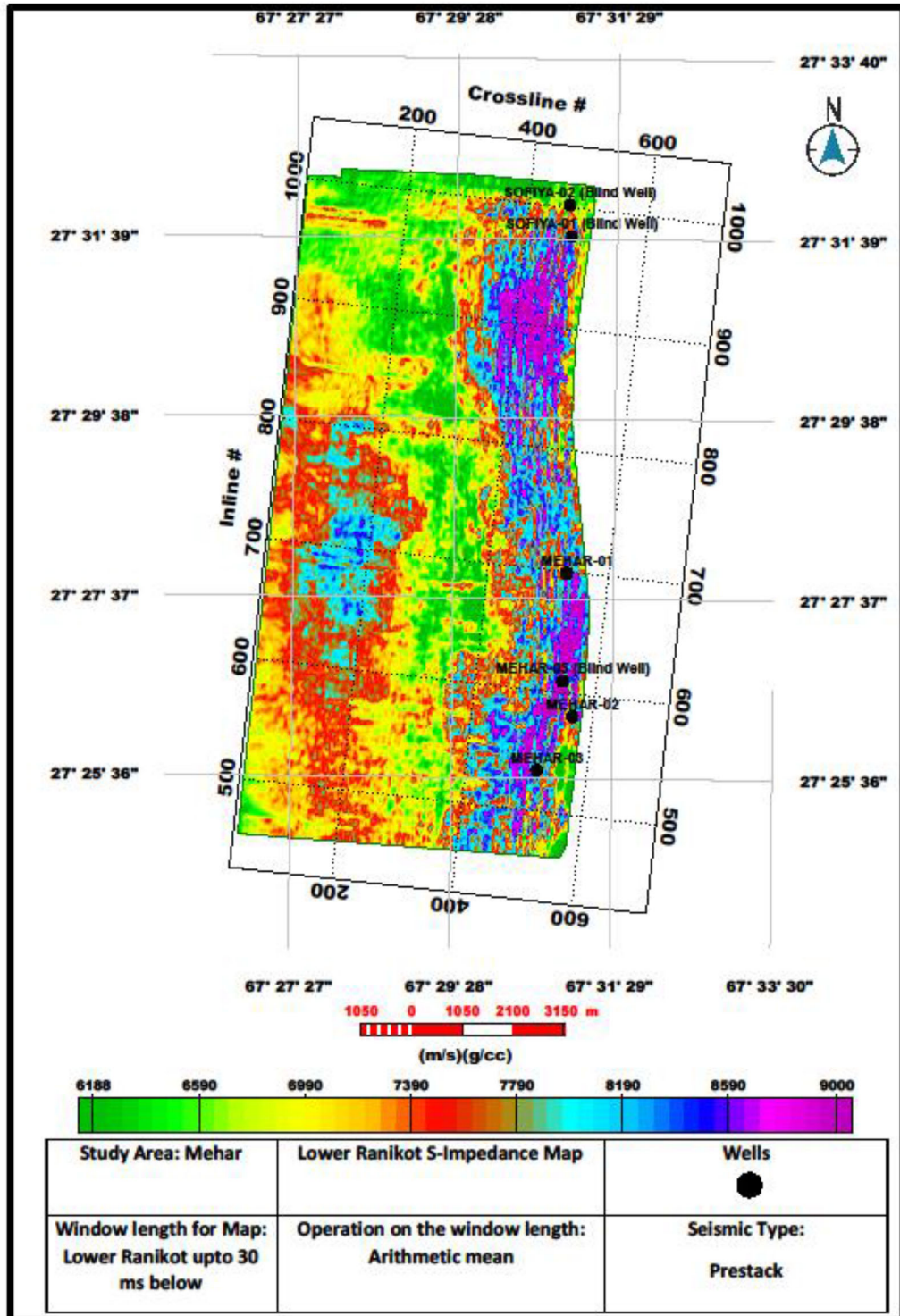


Figure 18

Arithmetic mean of Z_s using PSSI at Lower Ranikot, with a window of 30 ms below the interpreted horizon

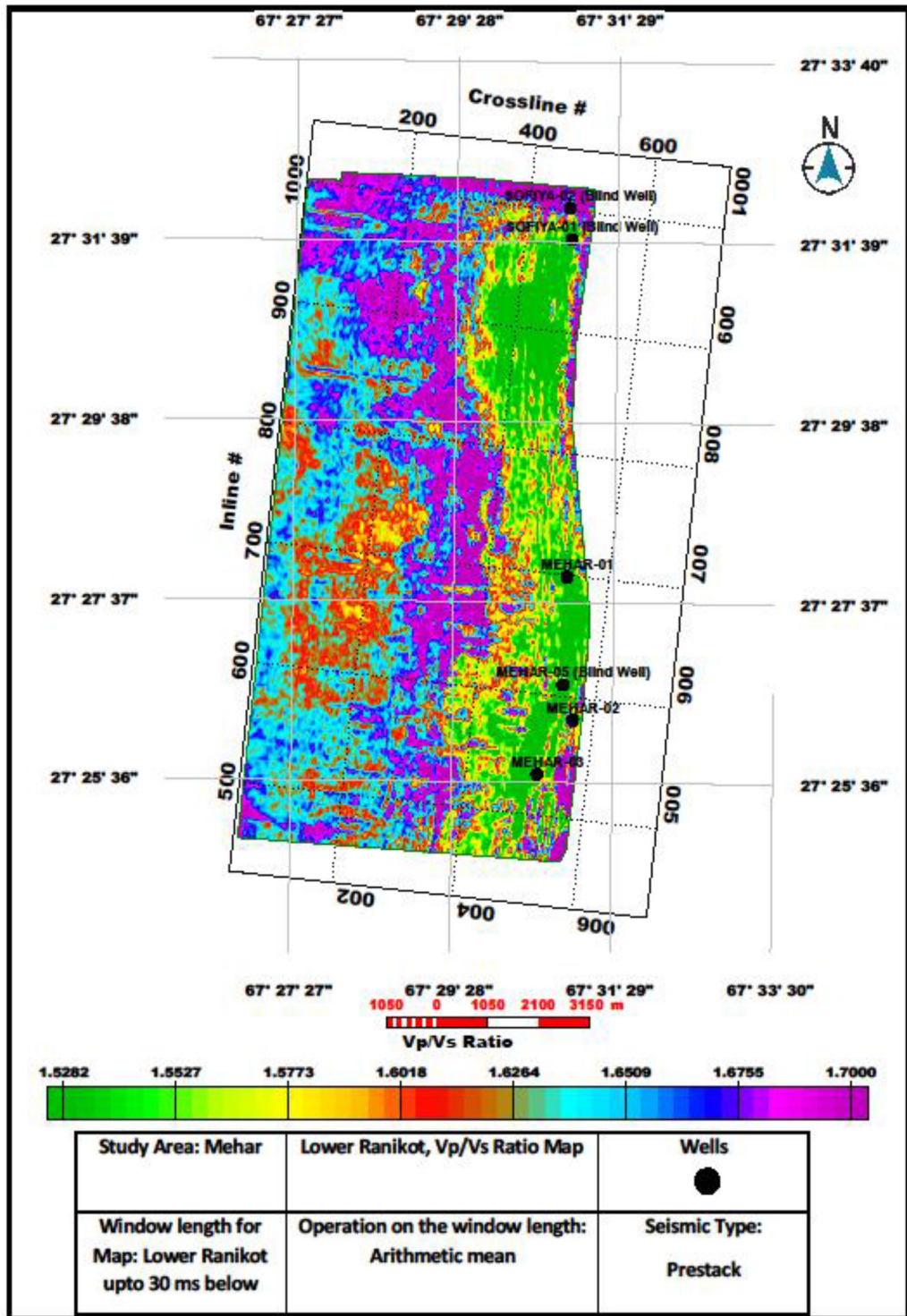


Figure 19

Arithmetic mean of Vp/Vs using PSSI at Lower Ranikot, with a window of 30 ms below the interpreted horizon

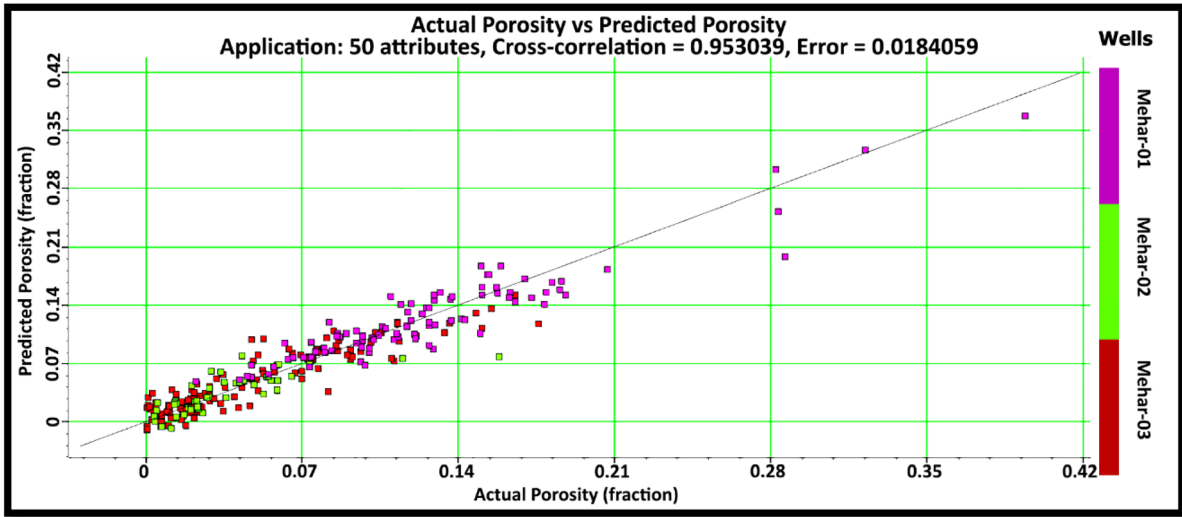


Figure 20
PNN analysis for the prediction of porosity in the study area

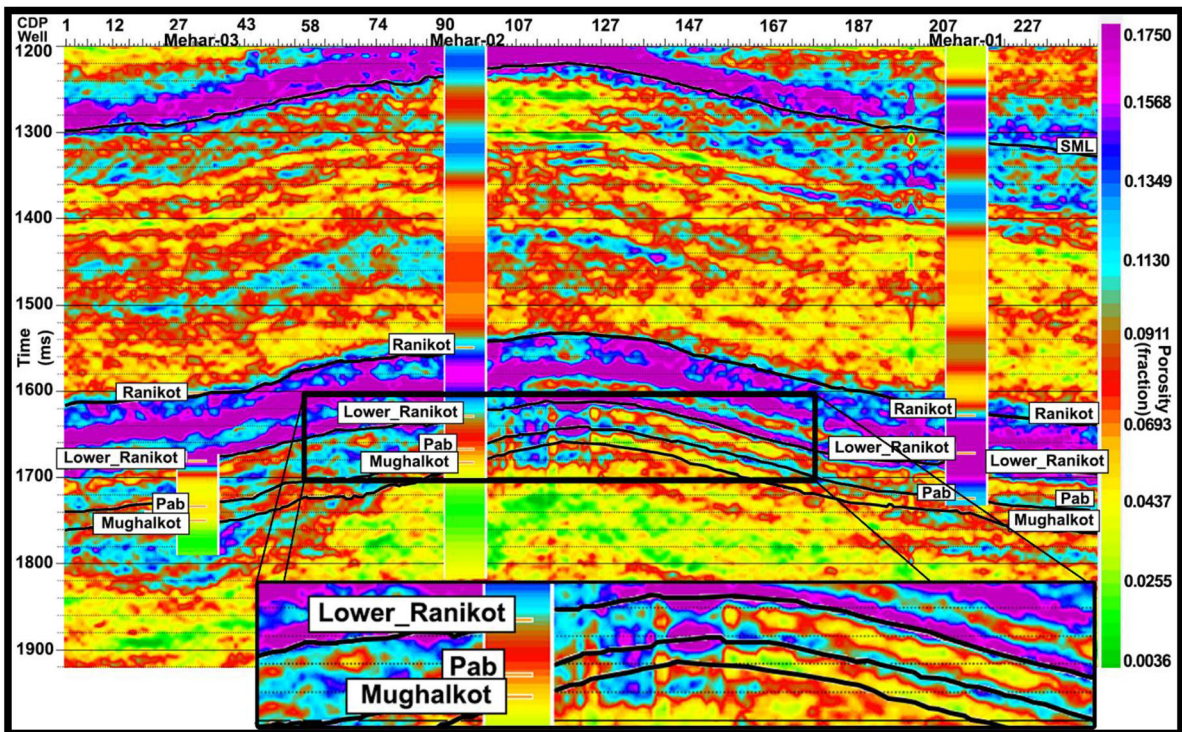


Figure 21
Arbitrary line of inverted porosity volume passing through the wells (Mehar-01, 02, and 03) with overlaid porosity logs. The zone around Mehar-02 is zoomed in for better visualization

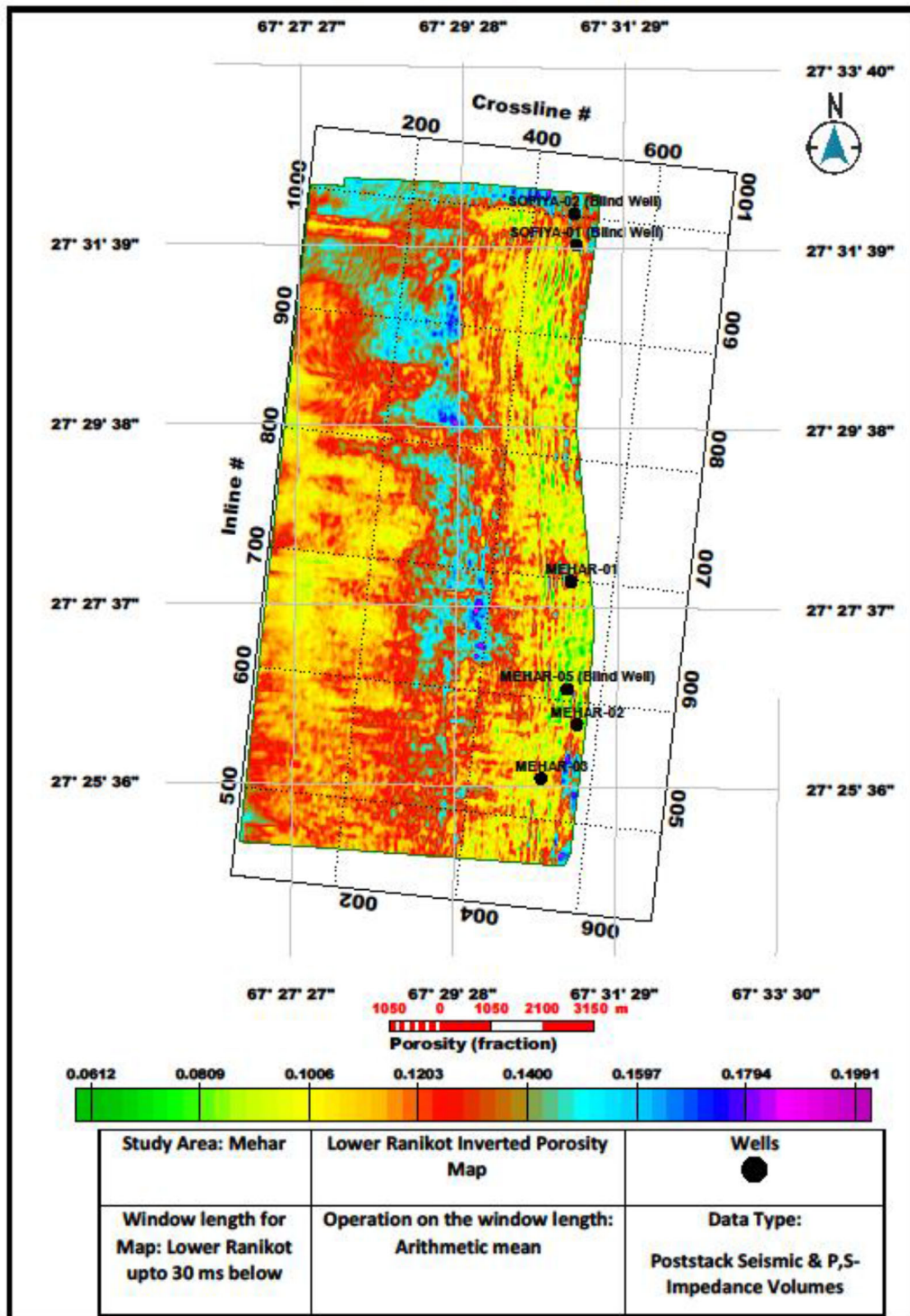


Figure 22
Arithmetic mean of inverted porosity at Lower Ranikot, with a window of 30 ms below the interpreted horizon

Acknowledgements

All the authors would like to thank the Directorate General of Petroleum Concessions (DGPC), Pakistan, for providing the data for this research work. The authors would also like to thank the Department of Earth Sciences, Quaid-i-Azam University (QAU), Islamabad, Pakistan, Department of Earth and Environmental Sciences, Bahria University, Islamabad, Pakistan, Landmark Resources (LMKR), Pakistan, and CGG (HampsonRussell) for providing the necessary software and laboratory support to complete this work.

Publisher's Note Springer Nature remains neutral with regard to jurisdictional claims in published maps and institutional affiliations.

REFERENCES

- Adeoti, L., Adesanya, O. Y., Oyedele, K. F., Afinotan, I. P., & Adekanle, A. (2018). Lithology and fluid prediction from simultaneous seismic inversion over Sandfish field, Niger Delta Nigeria. *Geosciences Journal*, 22(1), 155–169.
- Ahmad, N., Fink, P., Strurrock, S., Mahmood, T. & Ibrahim, M. (2004). Sequence stratigraphy as predictive tool in Lower Goru Fairway, Lower and Middle Indus platform, Pakistan. Proceedings of: PAPG-SPE Annual Technical Conference (pp. 85–104). 8–9 October 2004, Islamabad, Pakistan.
- Ahmad, A. & Ahmad, N. (2005). Paleocene petroleum system and its significance for exploration in the southwest Lower Indus Basin and nearby offshore of Pakistan. Proceedings of: Annual Technical Conference (pp. 1–22). November 28–29, Islamabad, Pakistan.
- Ahmad, N., Mateen, J., Shehzad, C. H., Mehmood, N., & Arif, F. (2012). Shale gas potential of lower cretaceous sembar formation in middle and lower Indus Basin Pakistan. *Pakistan Journal of Hydrocarbon Research*, 22, 51–62.
- Akhter, G., Ahmed, Z., Ishaq, A., & Ali, A. (2015). Integrated interpretation with Gassmann fluid substitution for optimum field development of Sanghar area, Pakistan: A case study. *Arabian Journal of Geosciences*, 8(9), 7467–7479.
- Aki, K., & Richards, P. G. (1989). *Quantitative Seismology: Theory and Methods*. W.H. Freeman & Co.
- Ali, A., Zubair, Hussain, M., Rehman, K., & Toqeer, M. (2016). Effect of shale distribution on hydrocarbon sands integrated with anisotropic rock physics for AVA modelling: a case study. *Acta Geophysica*, 64(4), 1139–1163.
- Ali, A., Alves, T. M., Saad, F. A., Mateullah, T., & Hussain, M. M. (2018). Resource potential of gas reservoirs in south Pakistan and adjacent Indian subcontinent revealed by post-stack inversion techniques. *Journal of Natural Gas Science and Engineering*, 49, 41–55.
- Anna, B., Susanne, G., & Peter, K. (2009). Porosity-preserving chlorite cements in shallow-marine volcanoclastic sandstones: evidence from Cretaceous sandstones of the Sawan gas field Pakistan. *AAPG Bulletin*, 93(5), 595–615.
- Arshad, K., Imran, M. & Iqbal, M. (2013). Hydrocarbon Prospectivity And Risk Analysis of An Under-Explored Western Kirthar Fold Belt of Pakistan. In Offshore Mediterranean Conference and Exhibition. Offshore Mediterranean Conference.
- Asquith, G. B., Krygowski, D. A., Henderson, S., & Hurley, N. (2004). *Basic Well Log Analysis* (p. 244). American Association of Petroleum Geologists.
- Azeem, T., Chun, W. Y., Khalid, P., Qing, L. X., Ehsan, M. I., Munawar, M. J., & Wei, X. (2017). An integrated petrophysical and rock physics analysis to improve reservoir characterization of Cretaceous sand intervals in Middle Indus Basin Pakistan. *Journal of Geophysics and Engineering*, 14(2), 212–225.
- Azeem, T., Chun, W. Y., Khalid, P., Ehsan, M. I., Rehman, F., & Naseem, A. A. (2018). Sweetness analysis of Lower Goru sandstone intervals of the Cretaceous age, Sawan gas field Pakistan. *Episodes Journal of International Geoscience*, 41(4), 235–247.
- Barone, A., & Sen, M. K. (2015). *Comparison of HTI and Orthorhombic Methods for Determining Fracture Density and Fracture Azimuth from 3D Seismic Data SEG Technical Program Expanded Abstracts 2015* (p. 2916). Society of Exploration Geophysicists.
- Bender, F. K., & Raza, H. A. (1995). *Geology of Pakistan* (3rd ed., pp. 11–63). Stuttgart: Gebrüder Borntraeger.
- Berger, A., Gier, S., & Krois, P. (2009). Porosity-preserving chlorite cement in shallow-marine volcanoclastic sandstones: Evidence from Cretaceous sandstones of the Sawan gas field Pakistan. *AAPG Bulletin*, 93(5), 595–615.
- Besse, J., & Courtillot, V. (1988). Palaeogeographic maps of the continents bordering the Indian Ocean since the Early Jurassic. *Journal of Geophysical Research*, 92, 11791–11808.
- Busch, B., Becker, I., Koehrer, B., Adelman, D., & Hilgers, C. (2019). Porosity evolution of two Upper Carboniferous tight-gas-fluvial sandstone reservoirs: Impact of fractures and total cement volumes on reservoir quality. *Marine and Petroleum Geology*, 100, 376–390.
- Çemen, I., Fuchs, J., Coffey, B., Gertson, R., & Hager, C. (2014). Correlating porosity with acoustic impedance in sandstone gas reservoirs: Examples from the Atokan sandstones of the Arkoma Basin, southeastern Oklahoma. Search and Discovery Article, 41255.
- Chi, X. G., & Han, D. H. (2009). Lithology and fluid differentiation using a rock physics template. *The Leading Edge*, 28(1), 60–65.
- Clochard, V., Delépine, N., Labat, K., & Ricarte, P. (2009). *Post-Stack versus pre-stack stratigraphic inversion for CO2 monitoring purposes: A case study for the saline aquifer of the Sleipner Field SEG Technical Program Expanded Abstracts* (pp. 2417–2421). Society of Exploration Geophysicists.
- Coléou, T., Bornard, R., Allo, F., & Freudenreich, Y. (2005). *Petrophysical Seismic Inversion SEG Technical Program Expanded Abstracts 2005* (pp. 1355–1358). Society of Exploration Geophysicists.
- Dorrington, K. P., & Link, C. A. (2004). Genetic algorithm/neural-network approach to seismic attribute selection for well-log prediction. *Geophysics*, 69, 112–122. <https://doi.org/10.1190/1.1649389>

- Doyen, P. M., De Buyl, M. H., & Guidish, T. M. (1989). Porosity from seismic data, a geostatistical approach. *Exploration Geophysics*, 20(2), 245.
- Durrani, M. Z. A., Talib, M., Ali, A., Sarosh, B., & Naseem, N. (2020). Characterization and probabilistic estimation of tight carbonate reservoir properties using quantitative geophysical approach: A case study from a mature gas field in the Middle Indus Basin of Pakistan. *Journal of Petroleum Exploration and Production Technology*, 10, 2785–2804.
- Eidsvik, J., Avseth, P., Omre, H., & Mukerji, T. (2004). Stochastic Reservoir characterization using prestack seismic data. *Geophysics*, 69(4), 978–993. <https://doi.org/10.1190/1.1778241>
- Emujakporue, G. O., & Ngwueke, M. I. (2013). Structural interpretation of seismic data from a xy field, onshore Niger Delta, Nigeria. *Journal of Applied Sciences and Environmental Management*, 17(1), 153–158.
- Fatti, J., Smith, G., Vail, P., Strauss, P., & Levitt, P. (1994). Detection of gas in sandstone reservoirs using AVO analysis: a 3D seismic case history using the geostack technique. *Geophysics*, 59, 1362–1376.
- Fitzsimmons, R., Buchanan, J., & Izzat, C. (2005). The role of outcrop geology in predicting reservoir presence in the Cretaceous and Palaeocene successions of the Sulaiman Range Pakistan. *AAPG Bulletin*, 89(2), 231–254.
- Gogoi, T., & Chatterjee, R. (2019). Estimation of petrophysical parameters using seismic inversion and neural network modeling in Upper Assam basin India. *Geoscience Frontiers*, 10(3), 1113–1124.
- Haider, B. A., Aizad, T., Ayaz, S. A., & Shoukry, A. (2012). A comprehensive shale gas exploration sequence for Pakistan and other emerging shale plays. *SPE/PAPG Annual Technical Conference*, 10, 401–408.
- Hampson, D., Schuelka, J. S., & Quirein, J. A. (2001). Use of multiattribute transforms to predict log properties from seismic data. *Geophysics*, 66, 220–236. <https://doi.org/10.1190/1.1444899>
- Hampson, D. P., Russell, B. H., & Bankhead, B. (2005). *Simultaneous Inversion of Pre-stack Seismic Data SEG Technical Program Expanded Abstracts*. Society of Exploration Geophysicists.
- Helgesen, J., Magnus, I., Prosser, S., Saigal, G., Aamodt, G., Dolberg, D., & Busman, S. (2000). Comparison of constrained sparse spike and stochastic inversion for porosity prediction at Kristin Field. *The Leading Edge*, 19(4), 400–407.
- Hinsch, P., Asmar, C., Hagedorn, P., Nasim, M., Rasheed, M. A., Stevens, N., Bretis, B. & Kiely, J. M. (2018). Structural Modelling in the Kirthar Fold Belt of Pakistan: From Seismic to Regional Scale. AAPG Search and Discovery Article (30546). <http://www.geoexplor.com/articles/2014/06/a-simple-guide-to-seismic-inversion>
- Huang, R., & Liu, Z. (2013). Application of pre-stack simultaneous inversion in sandstone oil reservoir prediction. *Progress in Geophysics*, 1, 41.
- Hughes, P., Van, E. R., & Mesdag, P. (2008). Estimation of Hydrocarbons in-place by simultaneous (AVO) inversion, constrained by iteratively derived low frequency models. *Fugro-Jason AS, PO Box, 8034*, 4068.
- Kalkomey, C. T. (1997). Potential risks when using seismic attributes as predictors of reservoir properties. *The Leading Edge*, 16(3), 247–251. <https://doi.org/10.1190/1.1437610>
- Karbalaali, H., Shadizadeh, S. R. & Riahi, M. A. (2013). Delineating hydrocarbon bearing zones using elastic impedance inversion: a persian gulf example. *Iranian Journal of Oil & Gas Science and Technology* 2(2), 8–19. Retrieved from http://ijogst.put.ac.ir/article_3534.html
- Karim, S. U., Islam, M. D., Hossain, M. M., & Islam, A. M. (2016). Seismic reservoir characterization using model based post-stack seismic inversion: in case of fenchuganj gas field Bangladesh. *Journal of the Japan Petroleum Institute*, 59(6), 283–292.
- Khan, M. S., Masood, F., Ahmed, Q., Jadoon, I. A. K., & Akram, N. (2017). Structural interpretation and petrophysical analysis for reservoir sands of lower goru, miano area, Central Indus Basin, Pakistan. *International Journal of Geosciences*, 8, 379–392.
- Lee, J., Mukerji, T., & Tompkins, M. (2013). Statistical Integration of Time-Lapse Seismic and Electromagnetic Data with a PDF Upscaling Method Using Multi-Point Geostatistics. *SEG Technical Program Expanded Abstracts 2013* (pp. 4998–5003). USA: Society of Exploration Geophysicists.
- Li, L., Lei, X., Zhang, X., & Sha, Z. (2013). Gas hydrate and associated free gas in the Dongsha Area of northern South China Sea. *Marine and Petroleum Geology*, 39(1), 92–101.
- Liu, Z., & Liu, J. (1998). Seismic-controlled nonlinear extrapolation of well parameters using neural networks. *Geophysics*, 63, 2035–2041. <https://doi.org/10.1190/1.1444496>
- Lorenzen, R. (2018). Multivariate linear regression of sonic logs on petrophysical logs for detailed reservoir characterization in producing fields. *Interpretation*, 6, T543–T553. <https://doi.org/10.1190/INT-2018-0030.1>
- Lu, Z. H. O. U., Zhong, F., Jiachen, Y. A. N., Zhong, K., Yong, W. U., Xihui, X. U., Peng, L. U., Zhang, W., & Yi, L. I. U. (2020). prestack inversion identification of organic reef gas reservoirs of permian changxing formation in damaoping area, sichuan basin, sw china. *Petroleum Exploration and Development*, 47(1), 89–100.
- Mahmud, O. A., & Aziz, S. A. (2002). Sequence stratigraphic study of Pab sandstone, Mehar Block, Middle Indus Basin Pakistan. *Warta Geologi*, 28(5), 7.
- Miller, S. L., & Stewart, R. R. (1990). Effects of lithology, porosity and shaliness on P-and S-wave velocities from sonic logs. *Canadian Journal of Exploration Geophysics*, 26(1–2), 94–103.
- Moghanloo, H. G., Riahi, M. A., & Bagheri, M. (2018). Application of simultaneous prestack inversion in reservoir facies identification. *Journal of Geophysics and Engineering*, 15(4), 1376–1388.
- Nawaz, U. S. (2013). Acoustic and Elastic Impedance Models of Gullfaks Field by Post-Stack Seismic Inversion. (M. Sc. Thesis). Petroleum Engineering and Applied Geophysics, Norwegian University of Science and Technology.
- Nimmo, J. R. (2004). Porosity and pore size distribution. *Encyclopedia of Soils in the Environment*, 3(1), 295–303.
- Ødegaard, E., & Avseth, P. (2004). Well log and seismic data analysis using rock physics templates. *First Break*, 22, 37–43.
- Ogilvie, S. R., Isakov, E., & Glover, P. W. (2006). Fluid flow through rough fractures in rocks. II: A new matching model for rough rock fractures. *Earth and Planetary Science Letters*, 241, 454–465.
- Oliver, D. S., Reynolds, A. C., & Liu, N. (2008). *Inverse theory for petroleum reservoir characterization and history matching*. Cambridge University Press.

- Patriat, P., & Achache, J. (1984). Collision chronology and its implications for crustal shortening and the driving mechanisms of plates—India-Eurasia. *Nature*, 311, 615–621.
- Pendrel, J., Schouten, H., & Bornard, R. (2017). *Bayesian Estimation of Petrophysical Facies and Their Applications to Reservoir Characterization SEG Technical Program Expanded Abstracts 2017* (pp. 3082–3086). USA: Society of Exploration Geophysicists.
- Prskalo, S. (2007). Application of Relations between Seismic Amplitude, Velocity and Lithology in Geological Interpretation of Seismic Data. Retrieved from <https://www.researchgate.net/publication/228492276>
- Richard, H., Johan, W. & Johan, S. (2001). Sequence Stratigraphic and Tectonics in the Kirthar Fold belt, Pakistan. ATC Conference Proceedings, 61–72.
- Robinson, E. A., & Silva, M. T. (1978). *Digital Signal Processing and Time Series Analysis*. Holden-Day.
- Russell, B. (1999). *Comparison of post-stack seismic inversion methods SEG Technical Program Expanded Abstracts* (p. 10). Society of Exploration Geophysicists.
- Russell, B. & Hampson, D. (1991). A comparison of post-stack seismic inversion methods. 61st Annual International Meeting, SEG, Expanded Abstracts, 876–878.
- Sams, M., & Carter, D. (2017). Stuck between a rock and a reflection: A tutorial on low-frequency models for seismic inversion. *Interpretation*, 5(2), B17–B27.
- Sams, M., & Saussus, D. (2007). *Estimating uncertainty in reserves from deterministic seismic inversion: Petroleum geostatistics* (p. 17). EAGE.
- Sams, M., & Saussus, D. (2013). *Practical implications of low frequency model selection on quantitative interpretation results SEG Technical Program Expanded Abstracts 2013* (pp. 3118–3122). Society of Exploration Geophysicists.
- Sams, M., Millar, I., Satriawan, W., Saussus, D., & Bhattacharyya, S. (2011). Integration of geology and geophysics through geostatistical inversion: a case study. *First Break*. <https://doi.org/10.3997/1365-2397.2011023>
- Searle, M., Corfield, R., Stephenson, B., & McCarron, J. (1997). Structure of the North Indian continental margin in the Ladakh-Zaskar Himalayas: Implications for the timing of obduction of the Spontang ophiolite, India-Asia collision and deformation events in the Himalaya. *Geological Magazine*, 134(3), 297–316.
- Sinaga1, T.M., Rosid, M.S., Haidar, M.W., (2019). Porosity Prediction Using Neural Network Based on Seismic Inversion and Seismic Attributes. The 4th International Conference on Energy, Environment, Epidemiology and Information System (ICENIS 2019), E3S Web of Conferences 125, article no. 15006, 1–5. <https://doi.org/10.1051/e3sconf/201912515006>
- Swisi, A. (2009). Post and Pre-stack Attribute Analysis and Inversion of Blackfoot 3D Seismic Data Set. (M. Sc. Thesis). Geological Sciences, University of Saskatchewan, Saskatoon.
- Szeliga, W., Bilham, R., Schelling, D., Kakar, D. M., & Lodi, S. (2009). Fold and thrust partitioning in a contracting fold belt: Insights from the 1931 Mach earthquake in Baluchistan. *Tectonics*. <https://doi.org/10.1029/2008TC002265>
- Torres-Verdin, C., & Sen, M. K. (2004). *Integrated Approach for the Petrophysical Interpretation of Post-and Pre-Stack 3-D Seismic Data, Well-Log Data, Core Data*. US: University of Texas.
- Valzania, S., Kfoury, M., Grandis, M. G., Valdistorlo, A., Fanello, G., Guerra, L. & Sultan, M. A. (2011, January). Kadanwari Field: a Tight Gas Reservoir Study and a Successful Pilot Well Give New Life to an Exploited Field. In SPE EUROPEC/EAGE Annual Conference and Exhibition. Society of Petroleum Engineers.
- Yilmaz, Ö. (2001). *Seismic Data Analysis: Processing, Inversion, and Interpretation of Seismic Data*. Society of Exploration Geophysicists.
- Young, A.A., Lubis, L.A. and Ghosh, D.P. (2016). Application of Simultaneous Inversion Method to Predict the Lithology and Fluid Distribution in “X” Field, Malay Basin. In IOP Conference Series: Earth and Environmental Science (Vol. 38). DOI: <https://doi.org/10.1088/1755-1315/38/1/012007>.
- Zafar, Z. A., Shoaib, K., Afsar, F., Raja, Z. A., Tanveer, A. & Burley, S. D. (2018). A radical seismic interpretation re-think resolves the structural complexities of the Zamzama field, Kirthar Foredeep, Pakistan. PAPG/SPE Annual Technical Conference, December 2018, Islamabad.
- Zoeppritz, K. (1919). Earthquake waves VIII B. About reflection and passage of seismic waves through discontinuous surfaces. *Gottinger Nachr.*, 1, 66–84.
- Zoya, H., & Carlos, T. (2013). Inversion-based method for estimating total organic carbon and porosity and for diagnosing mineral constituents from multiple well logs in shale-gas formations. *Interpretation*, 1(1), T113–T123.